IEEE Access
Multidisciplinary | Rapid Review | Open Access Journal

Received June 16, 2019, accepted July 26, 2019, date of publication August 7, 2019, date of current version September 25, 2019.

Digital Object Identifier 10.1109/ACCESS.2019.2933717

Novel Hybrid Extraction Systems for Fetal Heart Rate Variability Monitoring Based on Non-Invasive Fetal Electrocardiogram

RENE JAROS, RADEK MARTINEK, RADANA KAHANKOVA, AND JIRI KOZIOREK

Department of Cybernetics and Biomedical Engineering, Faculty of Electrical Engineering and Computer Science, VSB—Technical University of Ostrava, 708 00 Ostrava, Czech Republic

Corresponding author: Rene Jaros (rene.jaros@vsb.cz)

This work was supported in part by the Ministry of Education of the Czech Republic under Project SP2019/85 and Project SP2019/118, and in part by the European Regional Development Fund of the Research Centre through the Advanced Mechatronic Systems Project within the Operational Programme Research, Development and Education under Project CZ.02.1.01/0.0/0.0/16_019/0000867.

ABSTRACT This study focuses on the design, implementation and subsequent verification of a new type of hybrid extraction system for noninvasive fetal electrocardiogram (NI-fECG) processing. The system designed combines the advantages of individual adaptive and non-adaptive algorithms. The pilot study reviews two innovative hybrid systems called ICA-ANFIS-WT and ICA-RLS-WT. This is a combination of independent component analysis (ICA), adaptive neuro-fuzzy inference system (ANFIS) algorithm or recursive least squares (RLS) algorithm and wavelet transform (WT) algorithm. The study was conducted on clinical practice data (extended ADFECGDB database and Physionet Challenge 2013 database) from the perspective of non-invasive fetal heart rate variability monitoring based on the determination of the overall probability of correct detection (ACC), sensitivity (SE), positive predictive value (PPV) and harmonic mean between SE and PPV (F1). System functionality was verified against a relevant reference obtained by an invasive way using a scalp electrode (ADFECGDB database), or relevant reference obtained by annotations (Physionet Challenge 2013 database). The study showed that ICA-RLS-WT hybrid system achieve better results than ICA-ANFIS-WT. During experiment on ADFECGDB database, the ICA-RLS-WT hybrid system reached ACC > 80 % on 9 recordings out of 12 and the ICA-ANFIS-WT hybrid system reached ACC > 80 % only on 6 recordings out of 12. During experiment on Physionet Challenge 2013 database the ICA-RLS-WT hybrid system reached ACC > 80 % on 13 recordings out of 25 and the ICA-ANFIS-WT hybrid system reached ACC > 80 % only on 7 recordings out of 25. Both hybrid systems achieve provably better results than the individual algorithms tested in previous studies.

INDEX TERMS Noninvasive fetal electrocardiography, independent component analysis (ICA), adaptive neuro fuzzy inference system (ANFIS), recursive least squares (RLS), wavelet transform (WT), ICA-ANFIS-WT, ICA-RLS-WT, hybrid methods, fetal heart rate variability monitoring, extraction systems.

I. INTRODUCTION

Before the advent of electronics in obstetrics and gynaecology, doctors had to rely on their senses and experience. One of the first methods to detect non-invasive fetal cardiac activity was to listen to (auscultation) heart sounds using a stethoscope [1]. In this way, only basic information such as indicative fetal heart rate (fHR), significant arrhythmias, or cardiac arrest could be obtained about fetal health [2]. With the development of electrical engineering, it was possible to switch to more advanced fetal health monitoring - electronic fetal monitoring (EFM) [3]. In the 1960s, cardiotocography (CTG) was introduced; this is a new method using the ultrasound principle that allows EFM while watching uterine contractions [4].

EFM breeds the possibility of continuous monitoring and, thus, early detection of symptoms of fetal hypoxia [5] and other life-threatening conditions. This has led to a significant reduction in neonatal mortality, as shown, for example, by the study presented by Chen et al. in [6]. CTG is currently

The associate editor coordinating the review of this manuscript and approving it for publication was Sunil Karamchandani.

technically sophisticated and forms an essential part of modern obstetrics for its simplicity, speed, non-invasiveness and painlessness [7]. Despite these innumerable advantages, however, it faces problematic reliability and accuracy. In addition, its great drawback is the fact that it does not provide any information about Beat to beat (BTB) variabilities [8]. This is mainly due to the methods that are used to reduce the number of signal loss episodes. These methods include, in particular, correlation methods based on signal periodicity analysis. Their use leads to significant averaging of instantaneous fHR values [8]. It is therefore not possible to detect rapid changes in fHR - so-called short-term variability (STV) [8], [9], which is important for the assessment of fetal health.

Cases, when fetal hypoxia is diagnosed falsely positively, pose a big problem. Many studies [10]–[16] blame CTG for the large increase in the number of Caesarean sections, which has provably increased since this method was put into practice. The acute caesarean section, as a very invasive surgical procedure, is a great burden for the woman's, as well as the child's, body compared to the natural mode of delivery. Many researches [17]–[19] show that it is not only a physical, but also mental, burden that can lead to post-traumatic stress. In addition, this type of delivery is associated with considerable economic losses for hospital facilities [20], [21].

Fetal electrocardiography is a monitoring technique based on electrical potential monitoring, manifesting cardiac activity, specifically in the form of a fetal electrocardiogram (fECG). Fetal ECG has been studied for over 100 years - it was first mentioned in the scientific literature as early as 1906, when Cremer presented the first record of an abdominal fECG [22]. However, significant progress in this area took place about 50 years later, mainly due to the work of three independent groups of scientists in London, Stockholm and Paris [1]. This led in particular to the first direct fECG recordings that were presented at the Mount Sinai Hospital meeting in 1956 [23]. This accelerated further research in this field, in particular, the investigation of fECG morphology, and the heart rate derived therefrom, and their changes in the case of pathological conditions [1]. These findings have led to a better understanding of the pathophysiology of the fetal cardiovascular system during childbirth and, thus, to recommendations for obstetricians used also for CTG monitoring [1].

The first attempts to capture the non-invasive fECG at the beginning of the 1960s were limited mainly by the technical possibilities at that time. Many authors [24]–[26] have been able to capture abdominal ECGs (aECGs) and describe them in relation to invasive recordings, but the major limitation was the large amount of interference that was sensed along with the useful signal, especially the maternal ECG (mECG). Although there were efforts to perform automatic reduction of the maternal component from the aECG, its complete elimination was not achieved [1].

The biggest problem with the reduction of the maternal component is the fact that the fECG signal overlaps in the time and frequency domain and, moreover, its amplitude is several times higher. Hence, classical linear filtration is ineffective in this respect and more advanced methods are required. With advances in computer technology and signal processing techniques, significant progress has been made in the extraction of fECG in recent decades. A large number of authors have achieved successful extraction using various methods and approaches, including:

1) Methods using only abdominal electrodes (AES methods) [27]–[65],
2) Methods using a combination of abdominal and thoracic electrodes (CS methods) [52], [66]–[89].

Healthcare professionals prefer the former, as it is clinically better feasible and more comfortable for the patient. Thus, most commercially available fECG-based devices use only abdominal measuring electrodes. At present, the main parameter in obstetrics is fHR. In this respect, a large number of AES algorithms have proven to be sufficient [32], [90], [91], leading to the implementation of the first commercially available NI-fECG-based systems in clinical practice in recent years [92], [93].

On the other hand, it should be noted that many authors have achieved very good results with adaptive methods using the CS approach [52], [66], [67], [71], [89]. As already mentioned, AES methods are useful for determining fHR obtained by detecting R-peaks of the ECG waveform. Nevertheless, processing by these methods generally distorts the fECG waveform, thus changing its morphology [94]–[96] (ST segment, QT interval, T/QRS ratio), which is important from a diagnostic perspective. From this perspective, adaptive CS methods are more effective. Therefore, combining both approaches is one way to improve the quality of fECG extraction. Examples of such research have been presented in [97], where hybrid methods based on combination of CS and AES algorithms appear to be the most effective methods, see [59], [98]–[102].

By developing new or improving existing methods of fECG monitoring, it could lead to both improved diagnosis of fetal hypoxia and minimized unnecessary Caesarean sections due to putative hypoxia. At the same time, the ST analysis of the ST section of the fECG waveform (STAN) is an available option, see [94]–[96]. This sophisticated method enables observation of the ST segment of the ECG waveform of the fetus, which is sensed transvaginally using a fetal scalp electrode (FSE). It is an invasive method that can only be used during delivery. An example of a device capable of performing ST analysis is, for example, STAN S31 made by the Swedish company Neoventa Medical AB [103].

The main challenge of current research is developing a system based on NI-fECG able to provide morphological analysis similar to the invasive ST analysis (i.e. NI-STAN). This paper proposed a method that, when optimized, would be able to achieve this task. To achieve this, it is necessary to find suitable algorithms in terms of both the extraction quality and the clinical feasibility, which is associated with both the performance and the computational cost.

Some of the authors tested the methods separately, some combined other methods. The results of studies [98]–[102]

show that hybrid methods outperform the other methods by means of the quality of the fECG extraction. The aim of the study proposed therein is combining the methods in order to combine their advantages and to eliminate their drawbacks. The approach of evaluating the results is also novel since we investigated the overall trend of the fHR curve in comparison with the reference FSE along with the standard evaluation by means of quality parameters such as accuracy (ACC), sensitivity (SE), positive predictive value (PPV), the harmonic mean between SE and PPV (F1), and so on.

The original contribution of this article is to test new hybrid methods combining independent component analysis (ICA), adaptive neuro-fuzzy inference system (ANFIS) algorithm, recursive least squares (RLS) algorithm and wavelet transform (WT) algorithm. Separately, these methods are relatively effective in fECG extraction [52], [66], [67], [71], [89]. Thus, their incorporation into the extraction and post-processing phases in a complex fully automated hybrid system seems very advantageous. Many authors have only tested their algorithms using synthetic data. However, the algorithm presented in this article has been verified on real clinical data - using the gold standard in the form of a signal continuously scanned with a FSE [104], [105].

The team of authors, as well as other research teams around the world in the past, tested both ICA and principal component analysis (PCA) [29], [51], [58], [98], [106] and adaptive systems using algorithms such as least mean squares (LMS) and RLS [69], [71], [107]–[109]. Based on the results supported by the statistical analysis, it can be stated that the robust hybrid system presented here achieves far better results in the determination of the fHR than the two aforementioned approaches alone. At the same time, this system is potentially able to extract the fECG waveform in such a way that a more detailed morphological analysis can be performed. This could lead to creating a new non-invasive alternative to the current STAN method.

Based on the in-depth research [97] and the initial experiments [58], [110] conducted, the ICA algorithm for the first part of the hybrid methods was selected. It has been found that the ICA algorithm is able to extract an mECG component from the aECG signals containing only the mECG signal and an aECG component containing the mECG signal and the fECG signal that is highlighted and is located at the same amplitude level as the mECG signal (marked as aECG*). Pre-processing of input aECG signals for adaptive algorithms thus forms an ICA algorithm. The mECG and aECG signals obtained after pre-processing are used as inputs to two different adaptive algorithms. These are ANFIS and RLS adaptive algorithms. The output fECG signal from both adaptive algorithms needs to be smoothed using WT (after fECG signal processing). The combination of these algorithms resulted in 2 hybrid methods, ICA-ANFIS-WT and ICA-RLS-WT. This chapter will deal with the 4 algorithms (ICA algorithm, ANFIS algorithm, RLS algorithm and WT algorithm) and their mathematical description.

A. INDEPENDENT COMPONENT ANALYSIS

This is an algorithm that tries to find a linear representation of non-Gaussian data that contains statistically independent components. When processing the fECG signal, the ICA algorithm principle can be easily explained. There are 2 electrodes located in the abdominal area of a pregnant woman providing 2 time signals: $x_1(t)$ and $x_2(t)$. These signals then include the sum of the signals induced by the maternal and fetal cardiac activity designated $s_1(t)$ and $s_2(t)$ (in reality, moreover, the noise-induced signals). In general, the composition of the signals $x_1(t)$ and $x_n(t)$ can be described by equations (1) and (2), where $\mathbf{A}_{\text{mix}}$ denotes a mixing matrix, a denote parameters depending on the distance of individual cardiac activities from the electrodes and n denotes the number of statistically independent components. The problem is that the parameters a are not known. The only possibility is to assume that the signals $s_1(t)$ and $s_2(t)$ are statistically independent, which is confirmed when processing the fECG signal. Equation (3) is then used to estimate independent components from mixed aECG signals, where $\mathbf{W}$ is the inverse matrix from the $\mathbf{A}_{\text{mix}}$ matrix [29], [58], [110]–[112].

$$x_{\text{j}} = a_{\text{j1}}s_1 + a_{\text{j2}}s_2 + \cdots + a_{\text{jn}}s_{\text{n}}. \tag{1}$$

$$\overrightarrow{x} = \mathbf{A}_{\text{mix}}\overrightarrow{s} = \sum_{\text{i=1}}^{\text{n}} a_{\text{i}}s_{\text{i}}. \tag{2}$$

$$\overrightarrow{s} = \mathbf{W}\overrightarrow{x}. \tag{3}$$

The most widely used type of ICA algorithm is the FastICA algorithm. It is based on a fixed iteration scheme looking for maxima of data not derived from $\overrightarrow{w}^{\text{T}}\overrightarrow{x}$ normal data distribution. To devise the FastICA algorithm, weight vector $\overrightarrow{w}$ and derivative g of the non-quadratic G function are needed. The FastICA algorithm is based on 4 steps. Before performing the following steps, pre-processing using centring must be applied to create data of zero mean value and whitening to create data vectors whose components are subsequently uncorrelated with unit scattering. Furthermore, the convergence criterion δ ($\delta = 0.00001$ is often used), the maximum number of iterations of the k_{ICA} cycle (often $k_{\text{ICA}} = 100$) and the number of ICA, n output components must be selected. The smallest recommended number of output components for fECG signal processing is $ICA, n = 3$. Convergence seeks to achieve practically zero scalar product between old and new vector values. First, random standardized initial weights of vector $\overrightarrow{w}^{\text{T}}\overrightarrow{x}$ are created. Then the current vector $\overrightarrow{w}^{+}$ is stored in vector $\overrightarrow{w}$, and the equation (4) is used to calculate the kurtosis, or the negentropy can be calculated in this step. Subsequently, the standardization is performed using equation (5). The last step checks whether the scalar product of the new vector $\overrightarrow{w}^{+}$ and vector $\overrightarrow{w}$ is smaller than the selected convergence criterion δ, and whether the cycle has been run more times than the maximum number of k_{ICA} iterations selected. If the condition is not met, the second and third steps of the FastICA algorithm are repeated [110], [112].

$$\overrightarrow{w}^{+} = E\{\overrightarrow{x}\, g(\overrightarrow{w}^{\text{T}}\overrightarrow{x})\} - E\{g'(\overrightarrow{w}^{\text{T}}\overrightarrow{x})\}\overrightarrow{w}. \tag{4}$$

$$\overrightarrow{w}^{+} = \frac{\overrightarrow{w}^{+}}{\|\overrightarrow{w}^{+}\|}. \tag{5}$$

B. RECURSIVE LEAST SQUARES FILTER

Adaptive algorithms calculate error $e(n)$ between the desired and real output of the adaptive algorithm using equation (6), where $d(n)$ is the desired output of the adaptive algorithm and $y(n)$ is the actual output of the adaptive algorithm. The adaptive algorithm attempts to adjust the filter coefficients $w(n)$ to achieve an output as much correlated as the desired one [71], [113].

$$e(n) = d(n) - y(n). \tag{6}$$

The RLS algorithm is based on recursive determination of weight coefficients, Kalman filter theory, time averaging and also on the LMS algorithm. The advantage of this algorithm is that it uses the values of previous error estimates and has very high performance in time-varying environments. The disadvantage then is that it has higher computing complexity and has stability problems. Its aim is to minimize the result of the objective function ξ, see equation (7), where n represents the external time index indicating the number of last values and k denotes the internal time index. The required output p can be expressed by equation (8), where λ denotes the forgetting factor being in the interval <0,1>. Most often, the forgetting factor ranges from 0.95 to 0.99. The forgetting factor λ serves for forgetting the previous values. It is desirable to make a compromise between trying to achieve parameter convergence using $\lambda = 1$ and between the ability to monitor the algorithm's sensitivity to changing parameters using $\lambda < 1$. The ideal solution to the problem is to use a variable forgetting factor [71], [113], [114].

$$\xi(n) = \sum_{\mathrm{k}=1}^{\mathrm{n}} p_{\mathrm{n}}(k) e_{\mathrm{n}}^{2}(k). \tag{7}$$

$$p_{\mathrm{n}}(k) = \lambda^{\mathrm{n-k}}. \tag{8}$$

From equation (7), it is clear that at a certain time n, all the values obtained since the start of the RLS algorithm must be available. This means that the number of values processed rises with increasing time and, therefore, the RLS algorithm is very memory intensive. To reduce the computational complexity, the N_{RLS} filter order is used, which indicates the final number of previous values processed [71], [113], [114].

This algorithm updates the current variables in each iteration cycle based on the state in the previous iteration. When implementing the RLS algorithm, it is possible to reduce the computational complexity (except for decreasing the order of the filter) by omitting the inverse matrix step, whose calculation is not necessary in practice. In the first step, the filter output is calculated using the input vector of the current iteration and using the filter weights obtained during the previous iteration, see equation (9), where the vector $\overrightarrow{x}(n)$ denotes the input signal. In the second step, the mean gain vector is calculated using equation (10) and (11). The third step solves equation (12), which determines the value of the estimation error. In the following step, the balance vector $\overrightarrow{w}(n)$ is updated using the estimation error value and the gain vectors, see equation (13). In the last step, the inverse matrix is calculated, see equation (14), and the pattern selection from the training set is terminated. In Figure 6, the RLS algorithm application block can be seen, where the λ parameter shows the forgetting coefficient and N_{RLS} indicates the filter order [71], [113], [114].

$$\overrightarrow{y}_{\mathrm{n-1}}(n) = \overrightarrow{w}^{\mathrm{T}}(n-1)\overrightarrow{x}(n). \tag{9}$$

$$\overrightarrow{u}(n) = \tilde{\Psi}_{\lambda}^{-1}(n-1)\overrightarrow{x}(n). \tag{10}$$

$$\overrightarrow{k}(n) = \frac{1}{\lambda + \overrightarrow{x}^{\mathrm{T}}(n)\overrightarrow{u}(n)}\overrightarrow{u}(n). \tag{11}$$

$$\overrightarrow{e}_{\mathrm{n-1}}(n) = d(n) - \overrightarrow{y}_{\mathrm{n-1}}(n). \tag{12}$$

$$\overrightarrow{w}(n) = \overrightarrow{w}^{\mathrm{T}}(n-1) + \overrightarrow{k}(n)\overrightarrow{e}_{\mathrm{n-1}}(n). \tag{13}$$

$$\tilde{\Psi}_{\lambda}^{-1}(n) = \lambda^{-1}\tilde{\Psi}_{\lambda}^{-1}(n-1) - \overrightarrow{k}(n)[\overrightarrow{x}^{\mathrm{T}}(n)\tilde{\Psi}_{\lambda}^{-1}(n-1)]. \tag{14}$$

C. ADAPTIVE NEURO FUZZY INFERENCE SYSTEM

This is the most commonly used adaptive algorithm to extract the fECG signal, developed by Jang in his work in 1993 [115]. This adaptive algorithm belongs to softcomputing methods, which are methods based on analytical methods, boolean logic, sharp classification, and deterministic search. The ANFIS algorithm can often be referred to as a hybrid adaptive algorithm because it combines a fuzzy inference system such as Takagi-Sugeno (fuzzy logic) [116], [117] and a feed-forward neural network learning algorithm [118], [119]. It is, therefore, a very powerful algorithm utilizing the advantage of fuzzy expert systems (the ability to work with inaccurate data) and neural networks (learning from the environment). In addition, the ANFIS algorithm can work with a learning algorithm consisting only of a backpropagation algorithm (BP) or a combination of BP and LMS algorithm [87], [120].

Thus, the ANFIS algorithm manifests itself as a fuzzy expert system implemented by a multilayer feed-forward neural network, and it is important to include Sugeno zero or first order model. Next, the system needs only one output, has no shared rules, the output membership functions are of the same type (linear or constant), and the number of rules correlates with the number of membership functions. Figure 5 shows the block diagram of the ANFIS algorithm. As the inputs of the noise cancellation system using ANFIS algorithm, we use mECG a mECG*, which is mECG with a 1 sample delay that is necessary for a correct estimation of the maternal component from the aECG* signal. It can be seen from the figure that the ANFIS algorithm architecture consists of 5 feed-forward layers. The ANFIS algorithm rule base can be described by two IF-THEN rules, see equations (15) and (16) [80], [87], [120].

$$R_1 : \text{IF } x \text{ is } A_1 \text{ and } y \text{ is } B_1, \quad \text{THEN } z_1 = p_1 X + q_1 Y + r_1. \tag{15}$$

$$R_2 : \text{IF } x \text{ is } A_2 \text{ and } y \text{ is } B_2, \quad \text{THEN } z_2 = p_2X + q_2Y + r_2. \tag{16}$$

In the 1st layer, which is adaptive and referred to as an input layer, fuzzification of input language variables representing individual nodes is performed. The functions for individual nodes can be written using equation (17). The neural network adapts, by its learning in the first layer, parameters of membership functions representing the antecedent. In the 2nd layer, which is called a rule layer, a multiplication of the first layer output signals is performed to determine the rules of weights w. The antecedent of rules is composed of language values of language variables. Thus, this layer consists of only non-adaptive nodes representing individual Takagi-Sugeno fuzzy rules. The weight of each rule is at the output of the 2nd layer and can be calculated using equation (18). The next layer represents the standardization layer composed only of non-adaptive nodes. The output of the 3rd layer is the ratio of the weights of individual rules to the sum of all rules. The standardized force of each rule is calculated using equation (19). The defuzzification layer (4th layer) uses adaptive nodes that have a linear or constant transmission function determined by the consequent. The 4th layer is connected to the standardization nodes as well as to the language variables x and y. The calculation of the adaptive nodes of the 4th layer is performed by equation (20), where p, q and r represent the parameters of the consequent. The last, 5th layer, consists of one non-adaptive node called summation, which uses equation (21) to determine ANFIS [80], [87], [120].

$$o_{1,\mathrm{i}} = \mu_{\mathrm{A_i}}(x).$$
$$o_{1,\mathrm{i}} = \mu_{\mathrm{B_i}}(y). \tag{17}$$
$$o_{2,\mathrm{i}} = w_\mathrm{i} = \mu_{\mathrm{A_i}}(x) \cdot \mu_{\mathrm{B_i}}(y). \tag{18}$$
$$o_{3,\mathrm{i}} = \overline{w_\mathrm{i}} = \frac{w_\mathrm{i}}{w_1 + w_2}. \tag{19}$$
$$o_{4,\mathrm{i}} = \overline{w_\mathrm{i}} f_\mathrm{i} = \overline{w_\mathrm{i}} \cdot z\mathrm{i} = \overline{w_\mathrm{i}}(p_\mathrm{i}x + q_\mathrm{i}y + r_\mathrm{i}). \tag{20}$$
$$o_{5,\mathrm{i}} = \sum_\mathrm{i} \overline{w_\mathrm{i}} f_\mathrm{i} = \frac{\sum_\mathrm{i} w_\mathrm{i} f_\mathrm{i}}{\sum_\mathrm{i} w_\mathrm{i}}. \tag{21}$$

Correct functionality of the ANFIS algorithm is very often performed by a combination of suitably set nonlinear parameters of the 1st layer using the BP and appropriately set linear parameters of the 4th layer using the LMS algorithm. This hybrid combination of BP and LMS algorithm was also used in our study. At the output of the ANFIS algorithm, the total error between the ANFIS output and the desired output is calculated. The program ends when an optimally small total error is reached or when the number of selected epochs (iterations) is exceeded. This combination of the ANFIS algorithm using BP and the LMS algorithm includes forward and reverse run [80], [87], [120].

D. WAVELET TRANSFORM

It is a very similar algorithm as the Fourier transform, but its great advantage is that it is very effective in processing non-stationary signals and signals containing multiple components (such as fECG signal processing). The essence of the WT algorithm is to select the appropriate shape and, then, the width of the wavelet. Often, wavelet types such as Daubechies, Symlets, and Coiflet are used in fECG signal processing. The Daubechies wavelet type seems to be the most suitable [39], [121], so in this work, this wavelet is selected when performing R-peak detection and smoothing the resulting fECG signal. In case a wrong type of mother wavelet is used, the result of WT could be unsufficient. Indeed, it could cause distortion of the output signal leading to inaccurate R-peaks detection. Basically, this algorithm performs signal decomposition using the selected type and width of the maternal wavelet Ψ [46], [122].

When applying discrete WT (DWT), it is necessary to choose the type of maternal wavelet Ψ and the decomposition level n. In the first decomposition stage, the signal is decomposed by the Low-pass filter to one cA approximation component (containing the lower half of the frequencies and providing the overall signal trend) and by the high-pass filter to one detailed cD component (containing the upper half of the frequencies and providing additional fineness information). In the second decomposition stage, the approximation component of the signal is divided into another one approximation component and one detailed component. This is happening until the final selected degree of decomposition [46], [122].

Equation (22) is used to describe DWT, where $\Psi^*_{\mathrm{j,k}}$ is a complex conjugate function to the daughter wavelet $\Psi_{\mathrm{j,k}}$. The daughter wave, which is dilated and shifted, can be described by equation (23), where j is the number of wavelets needed to cover the maternal wavelet and k is the wavelet position over time. The reverse DWT contains, at its input, signal c composed of the last approximation component and of all the detailed components from the highest degree of decomposition to the lowest one, see equation (24), where n denotes the degree of decomposition chosen. This composite signal is adjusted by thresholding before the DTW is completed. With reverse DWT, convolution with reconstruction filters is applied. Equation (25) is used to calculate the inverse DWT [46], [122].

$$DWT(f) = F(j,k) = \hat{f}(j,k) = \int_{-\infty}^{\infty} f(t) \cdot \Psi^*_{\mathrm{j,k}}(t)dt. \tag{22}$$
$$\Psi_{\mathrm{j,k}}(t) = 2^{\frac{\mathrm{j}}{2}} \Psi(2^\mathrm{j} t - k). \tag{23}$$
$$c = cA_\mathrm{n} + cD_\mathrm{n} + cA_{\mathrm{n}-1} + \cdots + cA_1. \tag{24}$$
$$DWT^{-1}(F) = f(t) = \sum_{\mathrm{j,k}} c_{\mathrm{j,k}} \cdot \Psi_{\mathrm{j,k}}(t). \tag{25}$$

Thresholding removes part of the noise by setting the coefficients to zero. The coefficients representing the useful portion of the signal are left undamaged. Adaptive thresholding uses the calculation of the noise standard deviation σ in a floating window with the selected length l and the selected empirical constant K to calculate the empirical threshold λ, see equation (26). Subsequently, it is advisable to select soft thresholding. First, the coefficients having a value

smaller than the threshold value are set to zero. Thereafter, the remaining coefficients having a value greater than the threshold value are shifted to zero by the threshold size. Equation (27) shows soft thresholding where U denotes the data processed [46], [122]–[124].

$$\lambda_{j,k} = \sigma_{j,k} \cdot K. \tag{26}$$

$$D(U, \lambda) = sgn(U)max(0, |U| - \lambda). \tag{27}$$

II. EVALUATION PARAMETERS

Correct evaluation is vital to verify the accuracy of the proposed method. Various evaluation parameters are used among different studies, so it makes an objective comparison challenging. This chapter describes the evaluation parameters that were selected for the evaluation of the results in order to ensure objectivity and repeatability of the experiments.

A. DETERMINATION OF EXTRACTION ACCURACY

To determine the accuracy of the extraction of the fECG signal relative to the reference fECG signal, the use of parameters determining the true positive values (TP), false positive values (FP) and false negative values (FN) was chosen. The number of TPs indicates how many times the R-peak was determined by the detector in the extracted signal at certain signal locations where R-peaks are to be determined by reference. The TP determination interval was 50 ms left and 50 ms right of the reference annotations. This interval was determined based on a study by Billeci and Varanini in 2017 [125]. This interval then serves to determine the number of FNs. If, according to the reference annotation, an R-peak was to be a frequency in the given point of the signal, but it was not determined in the extracted fECG signal; this means omitting the R-peak while increasing the number of FNs. The number FP indicates the determination of R-peaks outside the intervals in which the R-peaks are located by reference. When displaying the variable of fHR over time. An example of TP, FP and FN determination can be seen in Chapter IV, Figure 11.

By means of the TP, FP and FN values obtained, ACC can be calculated using equation (28), which is an estimate of the probability of correct detection of the R-peak (TP) by the hybrid method used relative to the reference. Parameter SE can be calculated using equation (29), PPV can be calculated using equation (30) and F1 can be calculated using equation (31) [58], [125].

$$ACC = \frac{TP}{n} \cdot 100 = \frac{TP}{TP + FP + FN} \cdot 100\,(\%). \tag{28}$$

$$SE = \frac{TP}{TP + FN} \cdot 100\,(\%). \tag{29}$$

$$PPV = \frac{TP}{TP + FP} \cdot 100\,(\%). \tag{30}$$

$$F1 = 2 \cdot \frac{SE \cdot PPV}{SE + PPV} = \frac{2 \cdot TP}{2 \cdot TP + FP + FN} \cdot 100\,(\%). \tag{31}$$

B. BLAND-ALTMAN GRAPH

If, in statistics, the goal is to evaluate pairs of random variables (X_1, Y_1), (X_2, Y_2) to (X_n, Y_n), which form pairs of dependent observations, it is necessary to use pair tests when verifying the position. Such tests include the Bland-Altman graph. In the first step of the pair test, the difference $\overrightarrow{D}$ and the averages $\overrightarrow{M}$ between the pairs of random variables is calculated, see equations (32) and (33), where $\overrightarrow{X}$ is a vector of random variables obtained from the fHR reference variable over time, $\overrightarrow{Y}$ is a vector of random variables obtained from the estimated fHR variable over time using the test method, n is the number of elements of the individual vectors and i is the i-th element of the individual vectors. It can then be assumed that the quantities $(D_1, D2, \ldots, D_n)$ are statistically independent and have the same distribution with the mean value $\mu = \mu_1 - \mu_2$ [58], [126]–[128].

$$\overrightarrow{D} = (D_1, D_2, \ldots, D_n), \quad \text{where } D_i = X_i - Y_i. \tag{32}$$

$$\overrightarrow{M} = (M_1, M_2, \ldots, M_n), \quad \text{where } M_i = \frac{X_i + Y_i}{2}. \tag{33}$$

The standardized normal distribution is based on point $\mu \pm 1.96\sigma$ indicating the 97.5 % quantile of the normal distribution, where μ indicates the mean value and σ the standard deviation. Then, from equation (34) and the modification of this equation, see equations (35), (36) and (37), where P denotes the probability and z denotes the normal distribution quantile point, it follows that 95 % of the area of normal distribution lies in the interval $\mu \pm 1.96\sigma$. The mean value of μ and 1.96σ from the difference vector $\overrightarrow{D}$ is calculated on the basis of equations (38) and (39), where n is the total number of elements of the difference vector $\overrightarrow{D}$ and i is the i-th element of the vector $\overrightarrow{D}$ [58], [126]–[128].

$$P(z_{0.025} < \frac{\overrightarrow{D} - \mu}{\sigma} < z_{0.975}) = 0.95. \tag{34}$$

$$P(-z_{0.975} < \frac{\overrightarrow{D} - \mu}{\sigma} < z_{0.975}) = 0.95. \tag{35}$$

$$P(-1.96 < \frac{\overrightarrow{D} - \mu}{\sigma} < 1.96) = 0.95. \tag{36}$$

$$P(\mu - 1.96\sigma < \overrightarrow{D} < \mu + 1.96\sigma) = 0.95. \tag{37}$$

$$\mu = \frac{\sum_{i=1}^{n} D_i}{n}. \tag{38}$$

$$1.96\sigma = 1.96 \cdot \sqrt{\frac{\sum_{i=1}^{n} (D_i - \mu)^2}{n - 1}}. \tag{39}$$

To construct a Bland-Altman graph, first, the values of the vectors $\overrightarrow{D}$ and $\overrightarrow{M}$ are plotted, then the middle line marking the mean value μ and then the upper and lower limits of compliance (LoA) are plotted using two lines indicating $\mu \pm 1.96\sigma$ [58], [126]–[128].

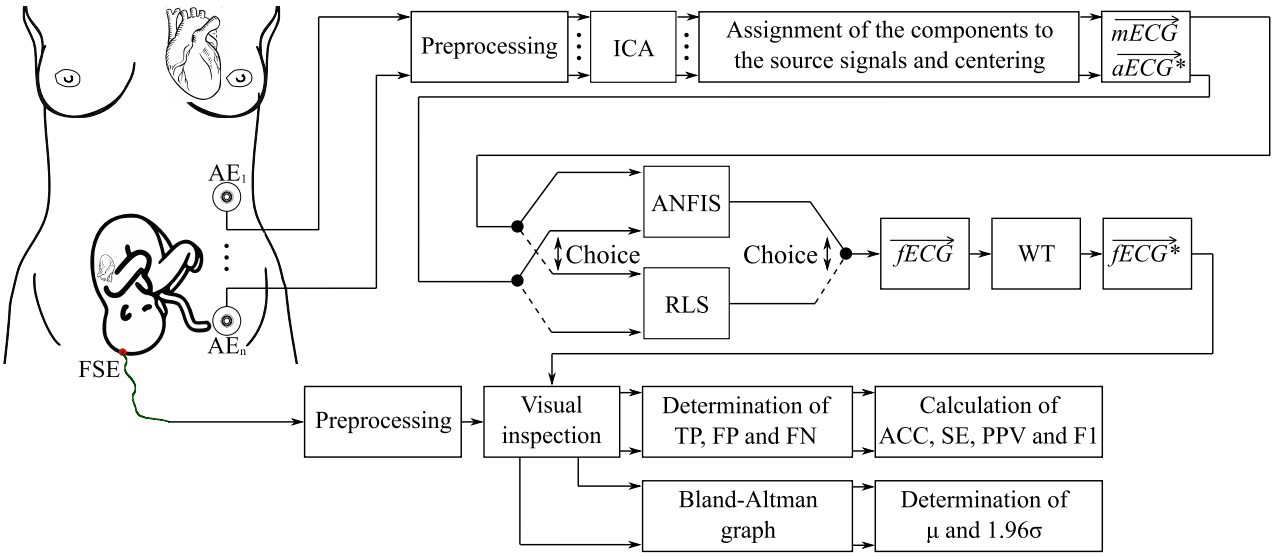

FIGURE 1. Block diagram of the hybrid system.

III. MATERIAL AND METHODS

In this chapter, the basic methods used in this article will be presented. This is a description of the dataset that was used to test the methods presented. Furthermore, both the hybrid extraction systems tested and the validation process are discussed in detail.

A. DATASET

In this work, a database of abdominal and direct fetal electrocardiogram (ADFECGDB) was used, which is a freely available database from Physionet sites [104], [105], [129]–[131]. This database contains 5 five-channel recordings from 5 different pregnant women in the 38th to 41st week of pregnancy which were taken at birth. All 5 recordings were taken at the pulmonary department of the Medical University of Zabrze, Poland. The individual signals are recorded with a bandwidth of 1 to 150 Hz (with 50 Hz network interference removed), a sampling rate of 1 kHz, a resolution of 16 bits and a length of 5 minutes. Individual recordings contain 4 aECG signals measured on the maternal abdomen and one fECG signal measured directly from the fetal head surface. 4 silver chloride electrodes placed around the navel (electrode surface was ground to reduce skin impedance), a reference electrode placed above the pubic symphysis, and an active electrode located on the left lower limb were used to measure aECG signals. The direct fECG signal was measured transvaginally using a typical spiral electrode. From the direct fECG signal measured, the positions of the R-peaks were automatically marked with the sensing system used and were subsequently verified by a group of cardiologists to compile accurate reference markers (annotations). In addition to the 5 recordings listed on the Physionet site (r01, r04, r07, r08, and r10), other 7 recordings (r02, r03, r05, r06, r09, r11, and r12) with sampling rate of 500 Hz were included in this study.

Another database used was set A of Physionet Challenge 2013 [131]. This database was created to improve the development of accurate fHR, fetal RR-interval, or fetal QT-interval estimation algorithms. Total of 25 records (a01 to a25) contain 4 aECG signals. The length of the individual signals is 1 minute with a sampling frequency of 1 kHz and a resolution of 12 bits. set A is consists of reference annotations that have been created and indicate the positions of the individual R-peaks.

B. HYBRID SYSTEM DESCRIPTION

This part describes in detail the concept of novel hybrid extraction systems for fHR variability monitoring based on NI-fECG. Subsequently, the modification of the fHR variable curves detected over time based on decision making and moving averaging used in all 12 recordings employed is described. Finally, a statistical comparison of the fHR variables estimated over time follows using two new hybrid methods of ICA-ANFIS-WT and ICA-RLS-WT against the fHR reference variable over time.

In Fig. 1, a block diagram of the hybrid system implemented can be seen. The methods employed consist of several steps which are performed successively to complete the successful extraction of the fECG signal. An example of extraction on the block diagram is shown on recording r01.

First, at least 2 measured aECG signals are fed to the preprocessing block where the initial signal adjustment is performed, see Fig. 2. The electrode layout in this figure is based on the ADFECGDB database [104], [105], [129]–[131]. The input signals are labelled as AE_1 to AE_4, the reference signal is denoted as AE_0 and the active ground is denoted as N. It is possible to select any filter of a certain band, but, in our case, the FIR filter was chosen. When using a bandpass filter, it is possible to set lower limit frequency $f_{\mathrm{FIR,L}}$, upper limit frequency $f_{\mathrm{FIR,U}}$, filter

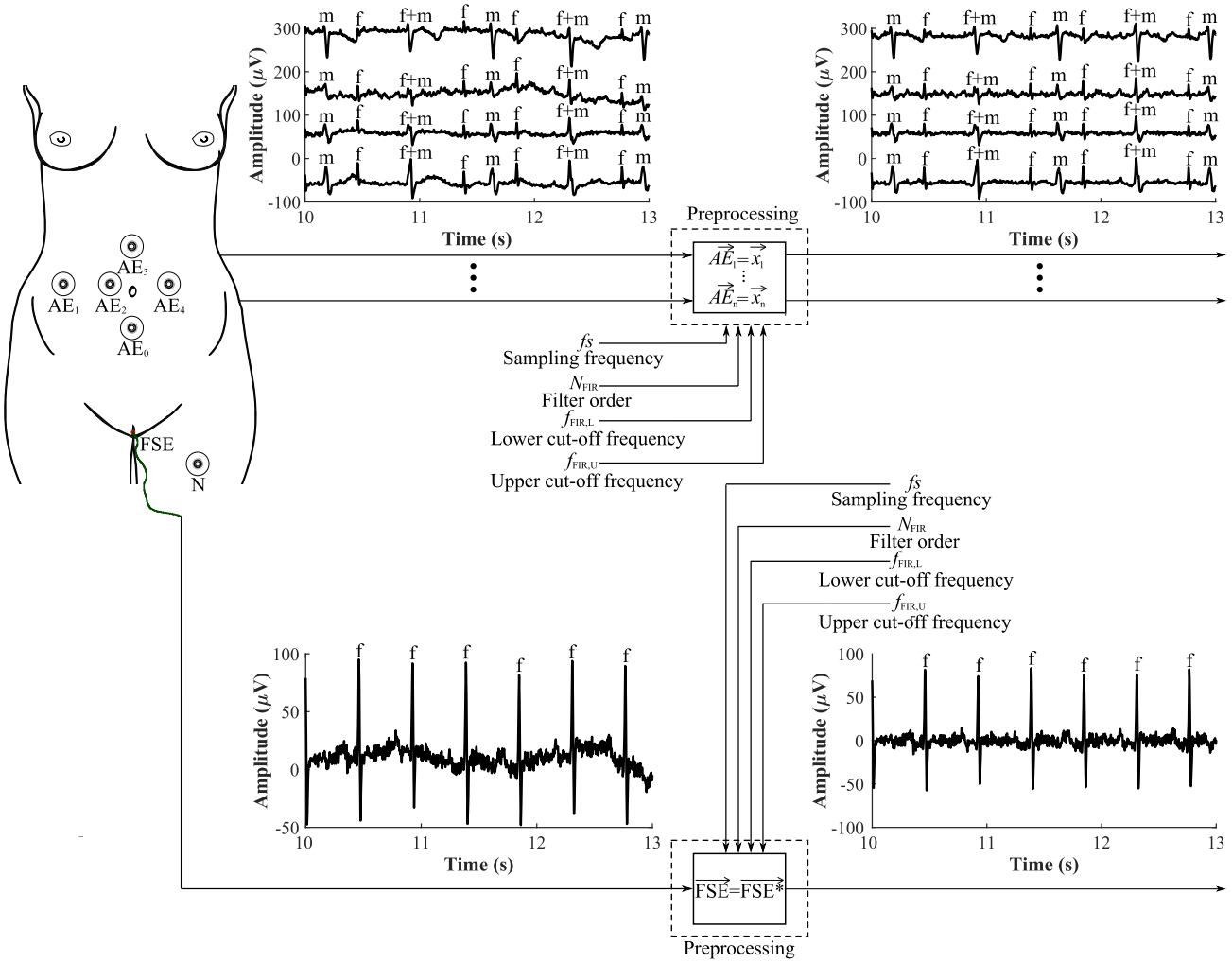

FIGURE 2. Input signal preprocessing.

order N_{FIR} and, in addition, it is necessary to set sampling frequency *fs* of the input aECG signals used. To adjust aECG signals, $f_{\mathrm{FIR,L}} = 3\,Hz$, $f_{\mathrm{FIR,U}} = 150\,Hz$, $N_{\mathrm{FIR}} = 500$ and $fs = 500; 1000\,Hz$ were set (5 recordingss from the ADFECGDB database had a sampling frequency of 1 kHz and 7 recordings had a sampling frequency of 500 Hz). The band selected cannot, in any way, damage the fECG signal because the fetal QRS complex is, according to the study by Sameni et al. in 2010 [132], in the range of 10 to 15 Hz. The FIR filter used with the bandpass set is designed to eliminate the variation of isolines, but also to remove noise, for example in the form of maternal and fetal movements.

Signals after preprocessing are then brought to the ICA algorithm block, see Fig. 3. In this block, the number of components *ICA*, *n*, the convergence criterion δ and the maximum number of iterations of the cycle k_{ICA} can be selected. $ICA, n = 3$, $\delta = 0.00001$, and $k_{\mathrm{ICA}} = 100$ were set for our experiments. The output of the ICA algorithm is then formed by 3 components. The scheme described shows that, in most cases, one component practically corresponds to the mECG signal, the second component corresponds to the aECG signal with the enhanced fECG signal at the same amplitude level as the mECG signal (marked as aECG*), and the third component corresponds to noise.

The individual components are in a different order each time the ICA algorithm is started, they have an altered amplitude due to standardization within the cycle, the components are rotated, and moreover, the components are time-shifted by several samples. For this reason, the output components are fed to an auto-centring block where the components are first differentiated and, then, rotated in the right direction, as shown in Fig. 4. Subsequently, the component corresponding to the mECG signal is amplitude and time aligned, based on the mQRS complexes, with the component corresponding to the aECG* signal with enhanced fECG signal. Finally, re-standardization is performed because amplitude adjustments occur during centring. If the automatic centring result is unsatisfactory, it is possible to use manual centring, where the user subjectively chooses the mECG signal and the aECG* signal with the fECG signal enhanced (or the

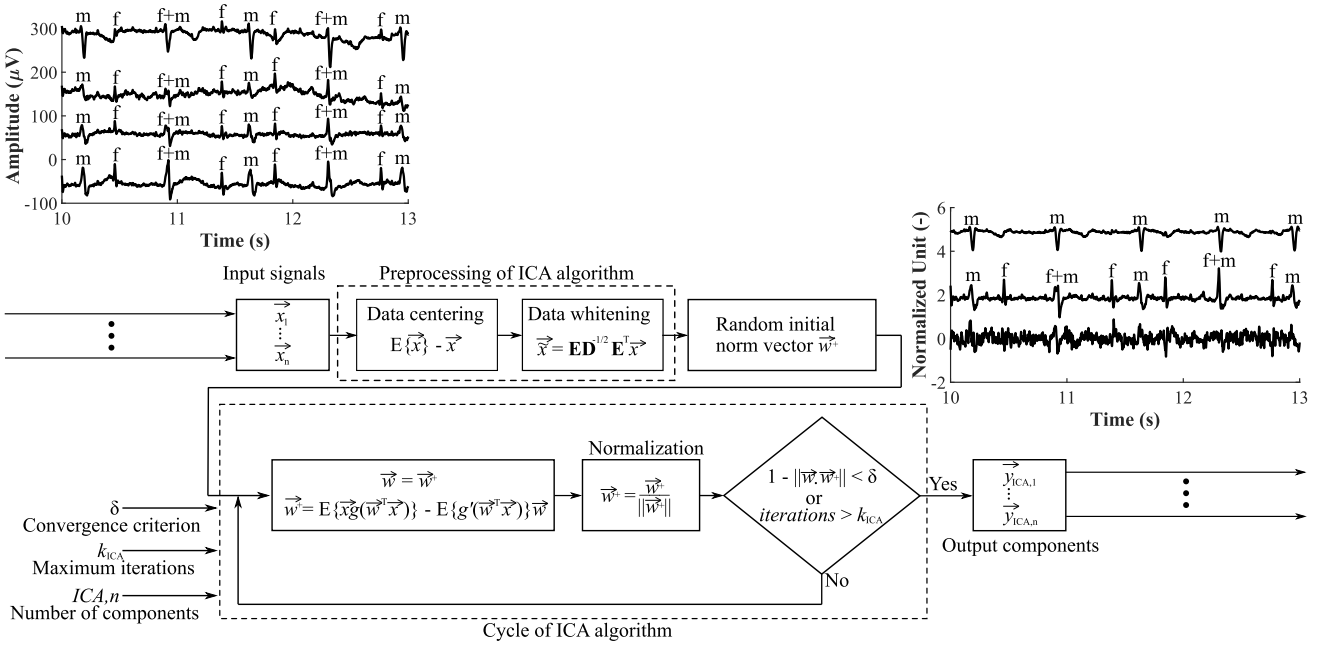

FIGURE 3. Implementation of the ICA algorithm to obtain components for adaptive systems.

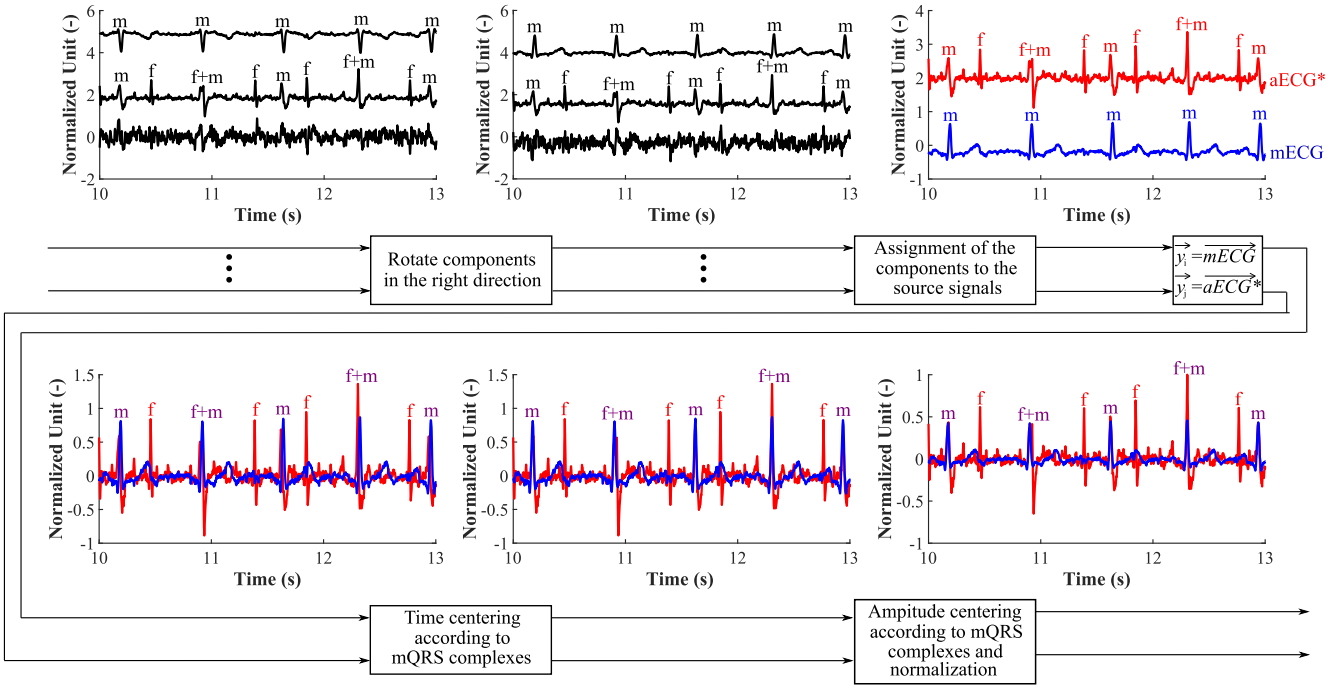

FIGURE 4. Progress of automatically selected algorithm and centring of output components from the ICA algorithm.

aECG signal can be selected from the input signals), and then the person aligns the signals by amplitude and time. After finishing the automatic or manual centring, the mECG signal and the aECG* signal are standardized. In the remaining course of the program, the output signals then have a dimensionless unit, and, thus, output fECG signals too.

Thus, the signals are ready for entering the adaptive algorithm and for the subsequent extraction of the fECG signal. It is now possible to select either the extraction of the fECG signal using the ANFIS algorithm, see Fig. 5, or the RLS algorithm, see Fig. 6. Using the ANFIS algorithm, it is possible to select the shape of membership functions μ_{ANF}, the number of membership functions ANF, n and the number

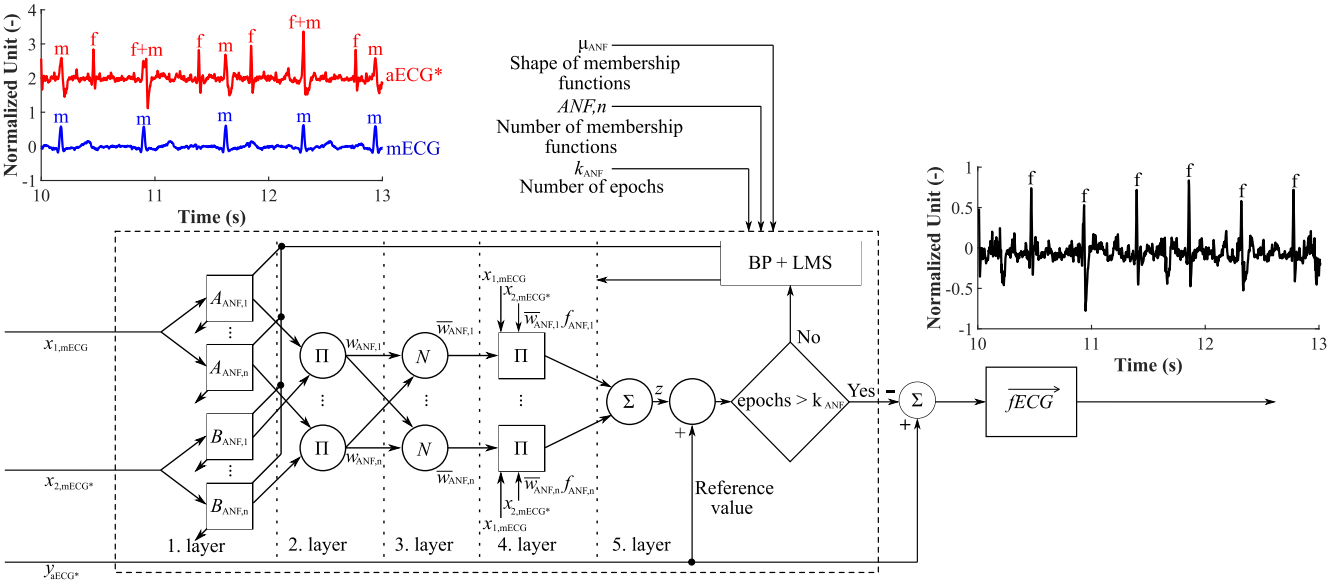

FIGURE 5. Extraction of the fECG signal from centred signals using the ANFIS algorithm.

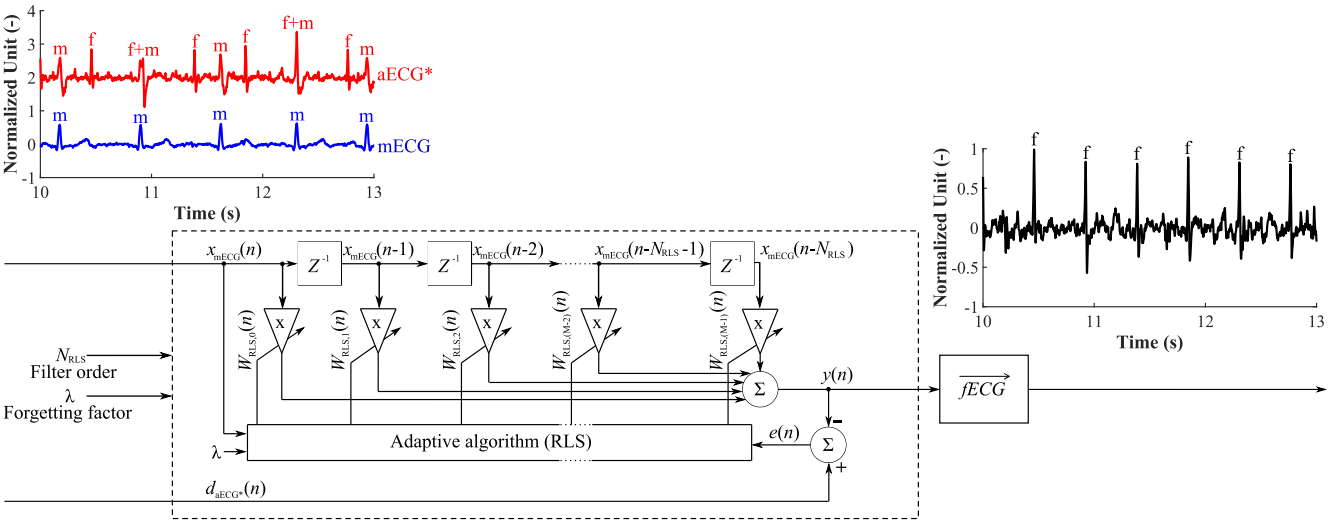

FIGURE 6. Extraction of the fECG signal from centred signals using the RLS algorithm.

of epochs k_{ANF}. As we mentioned before, hybrid combination of BP and LMS algorithm was used in our study. Conversely, when using the RLS algorithm, the N_{RLS} filter order and the forgetting coefficient λ must be selected. The advantage of this algorithm is the fact that it works faster than the ANFIS algorithm. In this work, the filter settings optimization was performed for both algorithms in order to achieve the highest accuracy of fECG signal extraction. In addition, we tested all possible combinations of input signals for each record. Altogether, 11 possible electrode combinations were tested for each record. In the case of ANFIS algorithm, we tested the settings such as the shape of the membership function: $\mu_{\mathrm{ANF}} = trimf$ (triangular membership function); $\mu_{\mathrm{ANF}} = trapmf$ (trapezoidal membership function); $\mu_{\mathrm{ANF}} = gbellmf$ (generalized bell membership function); $\mu_{\mathrm{ANF}} = gaussmf$ (Gaussian membership function); and also the number of membership functions: $ANF, n = 2$; $ANF, n = 4$; $ANF, n = 6$; $ANF, n = 8$; $ANF, n = 10$ and $k_{\mathrm{ANF}} = 10$; $k_{\mathrm{ANF}} = 20$; $k_{\mathrm{ANF}} = 30$. By combining the individual settings of the ANFIS algorithm, 45 outputs were generated for one electrode combination of a given record. A total of 660 outputs were generated for each record when applying the selected ANFIS settings to all 11 electrode combinations. Finally, the optimal setting of the ANFIS algorithm and the most appropriate combination of input signals for each record were found for each record as the global maximum of the ACC parameter. Table 1 shows the number of nodes, number of linear parameters, number of nonlinear parameters and

TABLE 1. ANFIS parameter setting with respect to the parameters of membership functions.

Number of mem. functions	Number of nodes	Number of linear parameters	Number of nonlinear parameters	Number of fuzzy rules
2	21	12	12	4
4	53	48	24	16
6	101	108	36	36
8	165	192	48	64
10	245	300	60	100

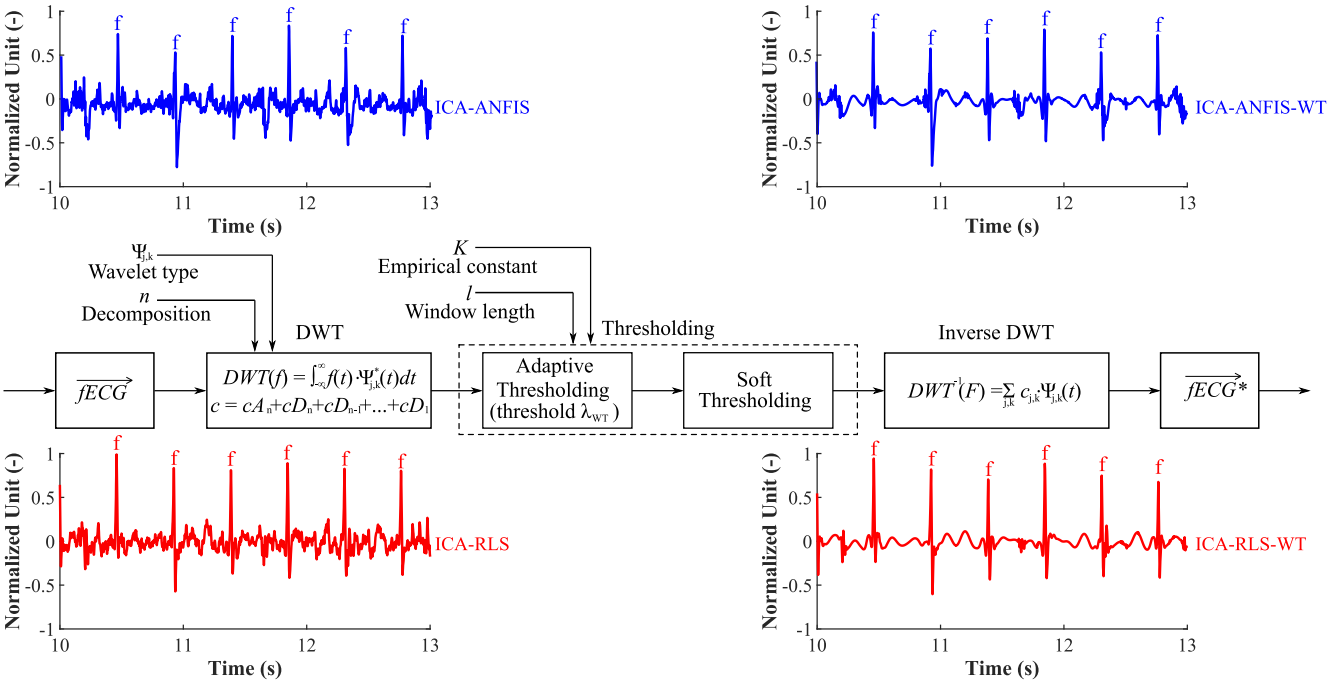

FIGURE 7. Smoothing the fECG signal using the WT algorithm after exiting the adaptive filter.

number of fuzzy rules when applying the selected number of membership functions ANF, n. A similar optimization approach was used to test the RLS algorithm, where the filter order N_{RLS} varied from 2 to 100 with step of 2. This way, 50 outputs of the RLS algorithm were generated for one electrode combination, i.e. 550 outputs for the whole record. Finally, the optimal setting of the RLS algorithm and the most appropriate combination of input signals for each record were found for each record.

The output fECG signals from the adaptive algorithms are initially re-standardized, and, then, they are adjusted (smoothed) in the last block using the WT algorithm. Fig. 7 shows the application of the WT algorithm where fECG is the input fECG signal labelled as ICA-ANFIS in the figure, if an adaptive ANFIS algorithm was applied in the previous step, or as an ICA-RLS, if an adaptive RLS algorithm was applied in the previous step. The output is fECG*, which is a smoothed fECG signal labelled as ICA-ANFIS-WT in the figure, if an adaptive ANFIS algorithm was applied in the previous step, or as an ICA-RLS-WT, if an adaptive RLS algorithm was applied in the previous step. The reason for smoothing the fECG signals is to highlight the R-peaks for the subsequent estimation of the fHR variable over time, which is the primary task of this work. For this algorithm, the type of maternal wavelet Ψ, the level of decomposition n, the length of the window l for adaptive thresholding and the empirical constant K are to be set. For the WT algorithm, $\Psi = db4$ (Daubechies mother wavelet with a width of 4), $n = 6$, $l = 500$ and $K = 2.5$ were set to test the fECG signal extraction accuracy.

The selection of all parameters was based on repeated testing of the individual algorithms on all recordings from the ADFECGDB database [104], [105], [129]–[131]. Many parameters have also been set based on the study of fECG signal processing using individual algorithms [55], [58], [70], [71], [97], [110], [113], [114].

The statistical evaluation of the fECG signal extraction quality relative to the reference can then be seen in Fig. 8, which illustrates a block scheme for plotting fHR variable curves over time, for plotting Bland-Altman graphs and for determining TP, FP, FN, μ, 1.96σ, ACC, SE, PPV and F1, see [58], [125], [128]. In the first step, the detection of R-peaks locations using a CWT-based detector is performed on the signals extracted, see [133]–[135]. The locations of

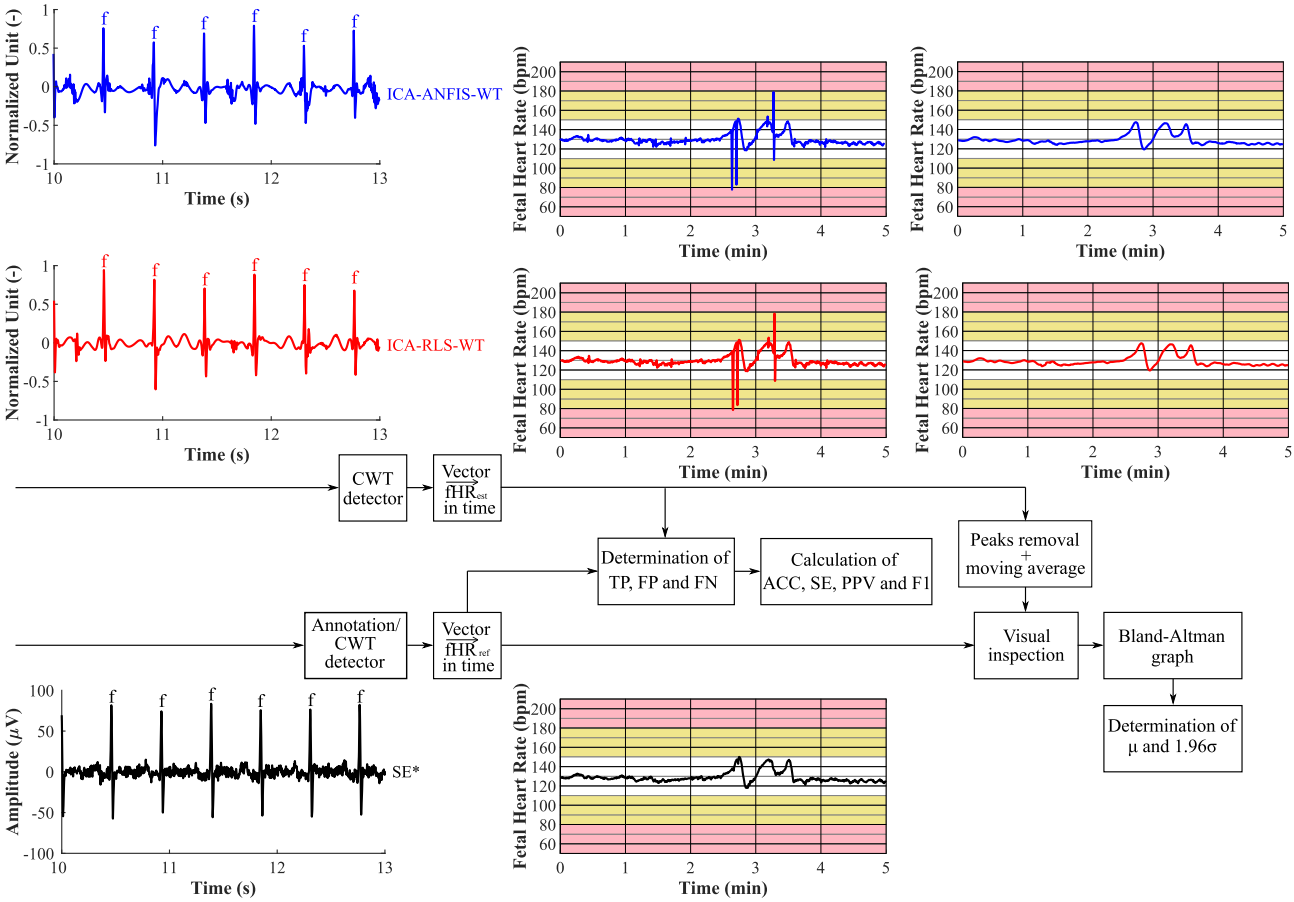

FIGURE 8. Diagram of extraction quality testing using both hybrid methods.

the R-peaks specified are used to determine the TP, FP and FN against the reference annotations (or the detected R-peaks in the reference signal to which reference annotations have not been provided). Subsequently, the calculation of ACC, SE, PPV and F1 is performed. In the next step, fHR variable curves over time are generated based on the locations of the R-peaks of the reference and extracted signals. The fHR variable curves of the signals extracted over time are first adjusted and then plotted in the graphs along with the fHR variable reference curve over time for visual evaluation. Subsequently, these curves are compared using Bland-Altman graphs and the mean values μ and 1.96σ are determined. A more detailed description of the detection and modification of the curves is provided in the following subchapter III-C.

C. DATA PREPARATION

Extraction of individual fECG signals using both hybrid methods is followed by estimation of fHR variable over time. First, the automatic determination (detection) of the R-peak locations from all extracted fECG signals is performed. The detector used is based on CWT, where the detector tries to find all local minima and maxima exceeding the specified threshold using Daubechies mother wavelet with a decomposition degree of 5. In the location where the distance between one local minimum and one local maximum is a maximum of 120 ms, the sample is recognized as an R-peak. It is a very accurate and effective detector. The locations of the R-peaks of the reference signals measured by FSE (hereinafter referred to as reference signals) are entered in the database for r01, r04, r07, r08 and r10 recordings; they are determined by medics and recognized as correct annotations of the recordings. There are no reference annotations for r02, r03, r05, r09, r11, and r12 recordings available, so it was necessary to perform accurate R-peak detection. Fig. 12 shows these reference signals in black. Using the reference signal R-peaks locations and the locations of the extracted signal determined, the TP, FP and FN values are then determined as described in subchapter II-A. An example of R-peaks annotations for the reference signal from r01 recording can be seen in Fig. 9a, and an example of R-peaks detection from the extracted fECG signal from r01 recording using the ICA-ANFIS-WT hybrid method can then be seen in Fig. 9b.

The next step was to determine the interval vector $\overrightarrow{T}$ between the individual locations of the R-peaks determined and, subsequently, to recalculate the interval vector $\overrightarrow{T}$ to the vector of the current fHR values $\overrightarrow{fHR}$ using equation (40), where n is the number of RR intervals determined. The result is multiplied by 60 to be in beats per minute (bpm),

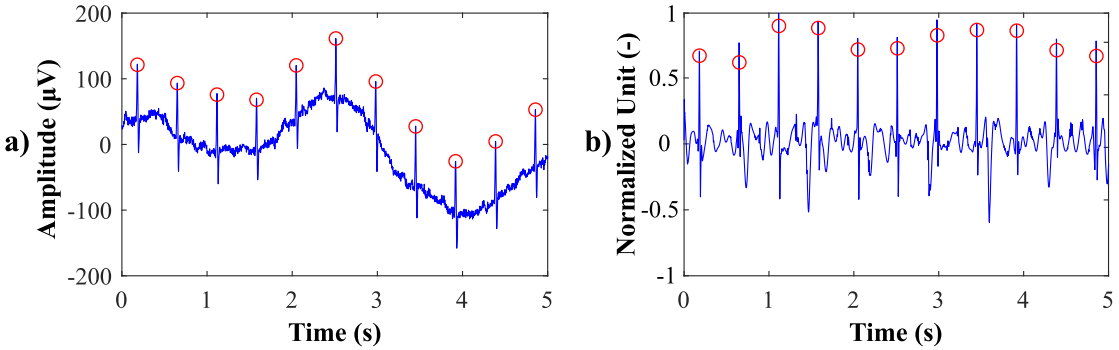

FIGURE 9. Examples of fECG signals from r01 recording with marked locations of R-peaks. a) a measured fetal scalp signal with an electrode marked with R-peaks on the basis of reference annotations; and b) an extracted signal using the ICA-ANFIS-WT method with R-peaks determined by the CWT detector.

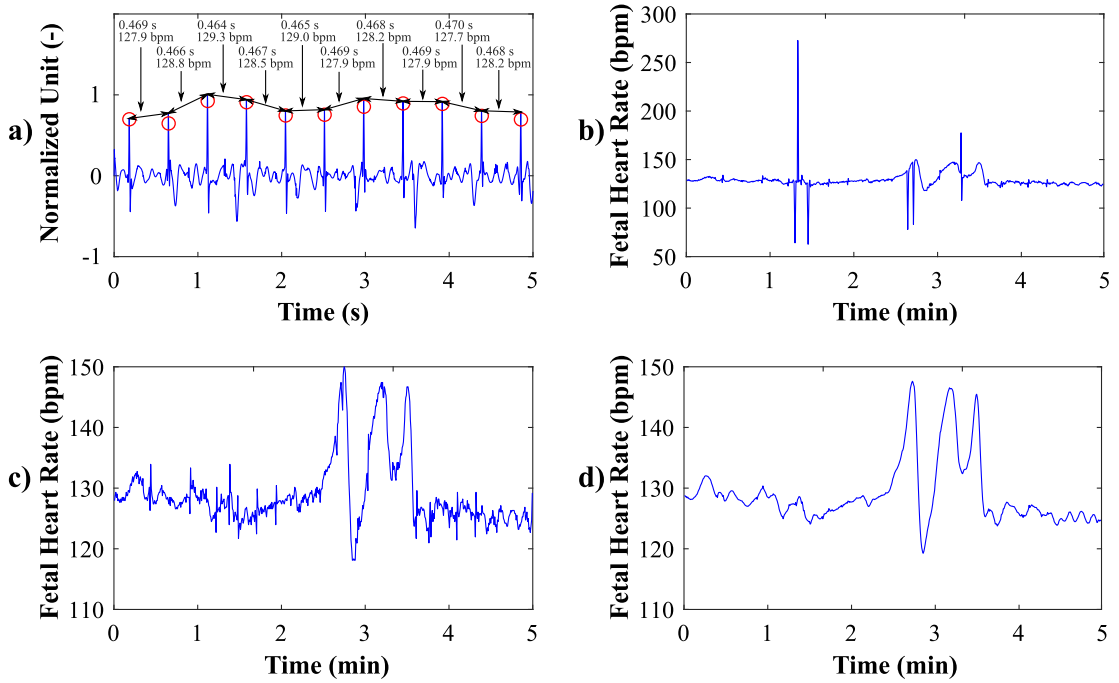

FIGURE 10. An example of how to estimate the fHR variable over time from the fECG signal extracted from r01 recording using the ICA-ANFIS-WT method. a) detecting R-peaks and creating a vector of current fHRs, b) plotting a vector of current fHRs in a graph, c) removing the deviated values by curve approximation, and d) performing moving averaging.

see Fig. 10a.

$$\overrightarrow{T} = (T_1, T_2, \ldots, T_n), \quad \overrightarrow{fHR} = (fHR_1, fHR_2, \ldots, fHR_n),$$

where

$$fHR_i = \frac{1}{T_i} \cdot 60. \tag{40}$$

The vector of current fHR plotted in the graph can be seen in Fig. 10b. It illustrates the fHR variable at the time of the fECG signal extracted using the ICA-ANFIS-WT method. In this figure, it can be seen that even the effective detector used estimates the R-peak incorrectly in some locations and deviated values occur. These values need to be eliminated as much as possible in order to achieve the most accurate fHR variable over time as it is the case of the reference signal. It should also be pointed out that the r01 recording in the figures is the best recording and the results herein were the best (in other recordings, the number of deviated values was much higher). The elimination of outliers was conducted using an algorithm that searches for these outliers and replaces them with curve approximation. The algorithm searches for locations where there is a big difference between the current fHR and the next fHR value. Such finding of the value is transferred to the average value calculated from the previous value before the outlier and the following value, which has been recognized as correct based on the decision process. The maximum number of consecutive outliers (either positively oriented, negatively oriented, or some positively and some negatively oriented) that can be removed by the algorithm is 5. A signal modified this way can be seen in Fig. 10c.

TABLE 2. Best combination of ANFIS algorithm settings when applying the hybrid method ICA-ANFIS-WT for each electrode set on recording r01 with the combination having the highest accuracy highlighted.

Combination of electrodes	Shape of membership functions	Number of membership functions	Number of epochs	TP	FP	FN	ACC (%)	SE (%)	PPV (%)	F1 (%)
1,2	gbellmf	2	20	621	9	23	95.10	96.43	98.57	97.49
1,3	trapmf	8	20	585	41	59	85.40	90.84	93.45	92.13
1,4	gaussmf	6	20	643	2	1	99.54	99.85	99.69	99.77
2,3	trapmf	6	10	404	82	240	55.65	62.73	83.13	71.50
2,4	gbellmf	10	10	624	12	20	95.12	96.89	98.11	97.50
3,4	gbellmf	2	10	584	49	60	84.27	90.68	92.26	91.46
1,2,3	gbellmf	2	30	611	22	33	91.74	94.88	96.52	95.69
1,2,4	trapmf	10	30	643	2	1	99.54	99.85	99.69	99.77
1,3,4	**gaussmf**	**2**	**10**	**643**	**1**	**1**	**99.69**	**99.85**	**99.85**	**99.85**
2,3,4	gaussmf	2	10	639	3	5	98.76	99.22	99.53	99.38
1,2,3,4	gbellmf	2	30	642	2	2	99.38	99.69	99.69	99.69

The last step in signal modification is to perform moving averaging, which is a time-based filtration. The filter slides on a moving window of the selected number of elements and averages. If a smaller number of eliminations of outliers than one fifth of the vector $\overrightarrow{fHR}$ elements were performed in the previous step, moving averaging of 10 elements is performed. Otherwise, moving averaging of 30 elements is performed. The final signal after moving averaging is shown in Fig. 10d. These signal modifications were made for all 12 fECG signals extracted obtained using both hybrid methods (together, 24 fECG signals extracted) and, after plotting the fHR variable curves over time, Bland-Altman graphs are created between the estimated curves and the fHR reference curves over time along with entering mean μ values and values 1.96σ.

It should be emphasized that, by plotting the reference annotations into the graph, it found that some contain several outliers. These outliers have been replaced in the annotations by the mean value between the previous and next correct value, since, otherwise, when executing the Bland-Altman graph, the determination of mean values μ and values 1.96σ was affected.

IV. RESULTS

The results in this chapter will be divided into 4 sections (experiments). Three experiments were carried out using signals from ADFECGDB database and one experiment was carried out using signals from database Physionet Challenge 2013. First, we perform optimization of the adaptive algorithms in order to find the most suitable combination of the filter settings and the electrodes to be used as the source of the inputs of the extraction systems (as described in chapter III-B). The signals that correspond to the most accurate extraction (according to the ACC parameter) are subsequently statistically analyzed and compared with the reference FSE signal. In the first part, the determination of TP, FP and FN (see chapter II-A) from all fECG signals extracted will be performed on 12 recordings from the ADFECGDB database using both hybrid methods and the ACC, SE, PPV and F1 parameters will be calculated to determine extraction accuracy. In the second part of this chapter, a visual representation of the estimated fHR variables adjusted over time will be performed for the reasons of a subjective assessment of the filtration accuracy relative to the fHR reference variables over time. The third part will deal with the implementation of Bland-Altman graphs to assess the accuracy of the fHR variable curve estimation over time relative to the fHR variable reference curves over time based on pair tests. Last part of this chapter deals with results of experiments carried out using signals from set A, Physionet Challenge 2013.

A. EVALUATION OF R-PEAK DETECTION ACCURACY

After performing optimization and associated extractions on all 12 recordings using both hybrid methods, the detection of R-peaks was performer using a CWT-based detector. Table 2 shows example of performed optimization by hybrid method ICA-ANFIS-WT on r01 recording. Similarly, this was performed for other recordings and for all recordings using the ICA-RLS-WT method. Based on the detected locations, the number of TP, FP and FN was determined for all signals extracted, see the methodology in Fig. 11.

By obtaining the individual numbers of TP, FP and FN for all signals extracted using both hybrid methods, the calculation of the selected parameters, ACC, SE, PPV and F1, was performed. The ACC parameter is evaluated as primary because other parameters cannot achieve less accuracy than the ACC parameter. It means, if the ACC parameter exceeds 95 %, the SE, PPV, and F1 parameters reach an accuracy of over 95 %. The results for the ICA-ANFIS-WT hybrid method can be seen in Table 3. It can be seen that the method worked, based on ACC, above 95 % with r01, r02, r05 and r08 recordings, value over 90 % for r09 recording, and over 80 % for r03 recording. On the basis of PPV and F1, it worked, moreover, above 95 % with r09 recording, which, according to the ACC and SE parameters, did not reach 95 % accuracy. This fact indicates that, in the signal extracted, on r09 recording, there was a low number of FP values, but a high number of FN values. With the other 6 recordings out of 12, this method did not achieve good results, and, thus, it was not, as an extraction method, effective in these recordings.

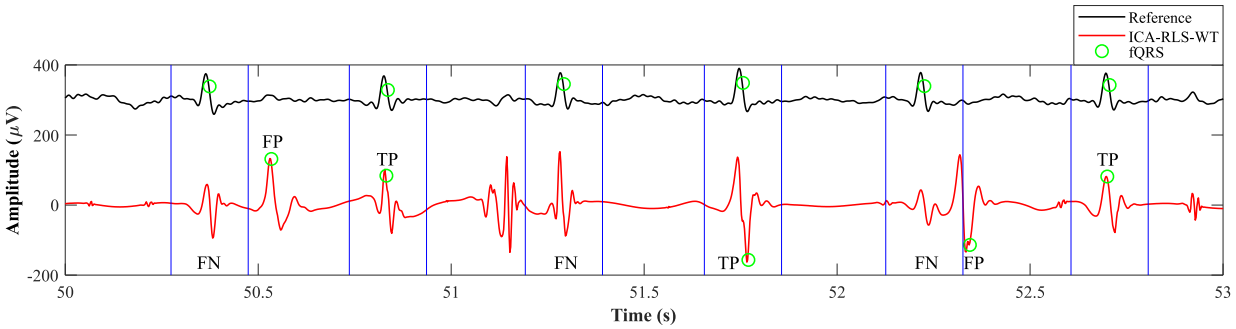

FIGURE 11. An example of automatic determination of TP, FP and FN based on reference annotations for the signal extracted using the ICA-RLS-WT method on r06 recording.

TABLE 3. Determination of TP, FP and FN based on the detection of R-peak locations in the fECG signals extracted from ADFECGDB database using the hybrid ICA-ANFIS-WT method relative to R-peak locations in the reference signal, and calculation of the ACC, SE, PPV and F1 parameters.

Recording	Combination of electrodes	Shape of membership functions	Number of membership functions	Number of epochs	Number of R-peaks by annotations	TP	FP	FN	ACC (%)	SE (%)	PPV (%)	F1 (%)
r01	1,3,4	gaussmf	2	10	644	643	1	1	99.69	99.85	99.85	99.85
r02	1,2,3,4	gbellmf	4	10	660	656	3	4	98.94	99.39	99.55	99.47
r03	2,4	gaussmf	6	30	684	618	49	66	84.31	90.35	92.65	91.49
r04	2,4	trimf	2	20	632	257	308	375	27.34	40.67	45.49	42.94
r05	1,4	gaussmf	4	20	645	633	4	12	97.54	98.14	99.37	98.75
r06	3,4	gbellmf	2	30	674	294	252	380	31.75	43.62	53.85	48.20
r07	1,3	trapmf	6	30	627	382	220	245	45.10	60.93	63.46	62.16
r08	1,4	gaussmf	2	10	651	650	1	1	99.69	99.85	99.85	99.85
r09	1,4	trapmf	2	20	657	622	15	35	92.56	94.67	97.65	96.14
r10	3,4	trimf	4	10	637	393	163	244	49.13	61.70	70.68	65.88
r11	1,4	gaussmf	10	30	705	260	324	445	25.27	36.88	44.52	40.34
r12	2,3	gbellmf	2	10	685	182	192	503	20.75	26.57	48.66	34.37

The same assessment was performed for the hybrid ICA-RLS-WT method and the results can be seen in Table 4. Based on the ACC parameter, this method achieved values above 95 % with r01, r02, r05, r08, and r09 recordings, values over 90 % for r03 and r10 recordings, and over 80 % for r06 and r07 recordings. With the signal extracted from r03 recording, the method, based on the PPV and F1 parameters, reached a values above 95 %. This fact indicates that, in the signal extracted, on r03 recording, there was a low number of FP values, but a high number of FN values. With the signal extracted from r10 recording, the method, based on SE and F1, reached a values above 95 %. It can be seen from the table that, in this recording, the method extracts signals, in which a low number of R-peaks are omitted during detection (FN), but it generates many FP values. With the other recordings, r04, r11, and r12, the ICA-RLS-WT hybrid method was not effective.

During this testing, the ICA-RLS-WT hybrid method achieved significantly better results than the ICA-ANFIS-WT hybrid method. It can be seen that, in 7 recordings out of 12, the ICA-RLS-WT hybrid method was able to extract fECG signals that reached at least 90 % based on the ACC parameter, and, as a result, with 9 recordings out of 12, they reached at least 80 % based on the ACC parameter. The ICA-ANFIS-WT hybrid method was able to extract usable fECG signals in only 6 recordings out of 12.

B. VISUAL COMPARISON

In this part of the evaluation of fECG signal extraction accuracy using both the hybrid methods tested, fHR variable curves over time were first generated for individually extracted signals. Subsequently, removal of outliers and sliding averaging for individual estimated fHR variables over time were performed. With the reference fHR variable curves over time given by annotations or detection by a CWT-based detector, removal of deviated values was also conducted in some cases. Consequently, the individual fHR variable curves over time obtained by the hybrid ICA-ANFIS-WT method are connected behind each other in a single graph together with the connected fHR variable curves over time given by the reference signals. Hence, the visual assessment of the accuracy of the estimate of the fHR variable curves over time using the ICA-ANFIS-WT method is shown in Fig. 12a. The same procedure is performed for the visual assessment of the accuracy of the estimate of the fHR variable curves over time using the ICA-RLS-WT method, see Fig. 12b. The graphical representation is based on FIGO classification [136]. The fHR segment from 110 to 150 bmp is labelled in white and indicates normal fHR. The segments from 150 to 180 bpm and from 90 to 110 bpm are marked in yellow and indicate an increased risk of fetal hypoxia. The segment above 180 and below 80 bpm is marked in pink and indicates that the fetus is at risk due to hypoxia, which may result in the need for

TABLE 4. Determination of TP, FP and FN based on the detection of R-peak locations in the fECG signals extracted from ADFECGDB database using the hybrid ICA-RLS-WT method relative to R-peak locations in the reference signal, and calculation of the ACC, SE, PPV and F1 parameters.

Recording	Combination of electrodes	Filter order	Number of R-peaks by annotations	TP	FP	FN	ACC (%)	SE (%)	PPV (%)	F1 (%)
r01	1,3,4	2	644	643	1	1	99.69	99.85	99.85	99.85
r02	1,2,3,4	16	660	656	1	4	99.24	99.39	99.85	99.62
r03	2,4	86	684	647	4	37	94.04	94.59	99.39	96.93
r04	1,4	46	632	528	67	104	75.54	83.54	88.74	86.06
r05	1,4	16	645	644	1	1	99.69	99.85	99.85	99.85
r06	1,2,3,4	98	674	592	43	82	82.57	87.83	93.23	90.45
r07	1,4	46	627	567	61	60	82.41	90.43	90.29	90.36
r08	1,4	30	651	650	1	1	99.69	99.85	99.85	99.85
r09	1,2,4	16	657	626	1	31	95.14	95.28	99.84	97.51
r10	1,2,3,4	52	637	626	33	11	93.43	98.27	94.99	96.61
r11	1,2,3,4	80	705	298	291	407	29.92	42.27	50.59	46.06
r12	1,2,3,4	100	685	584	48	101	79.67	85.26	92.41	88.69

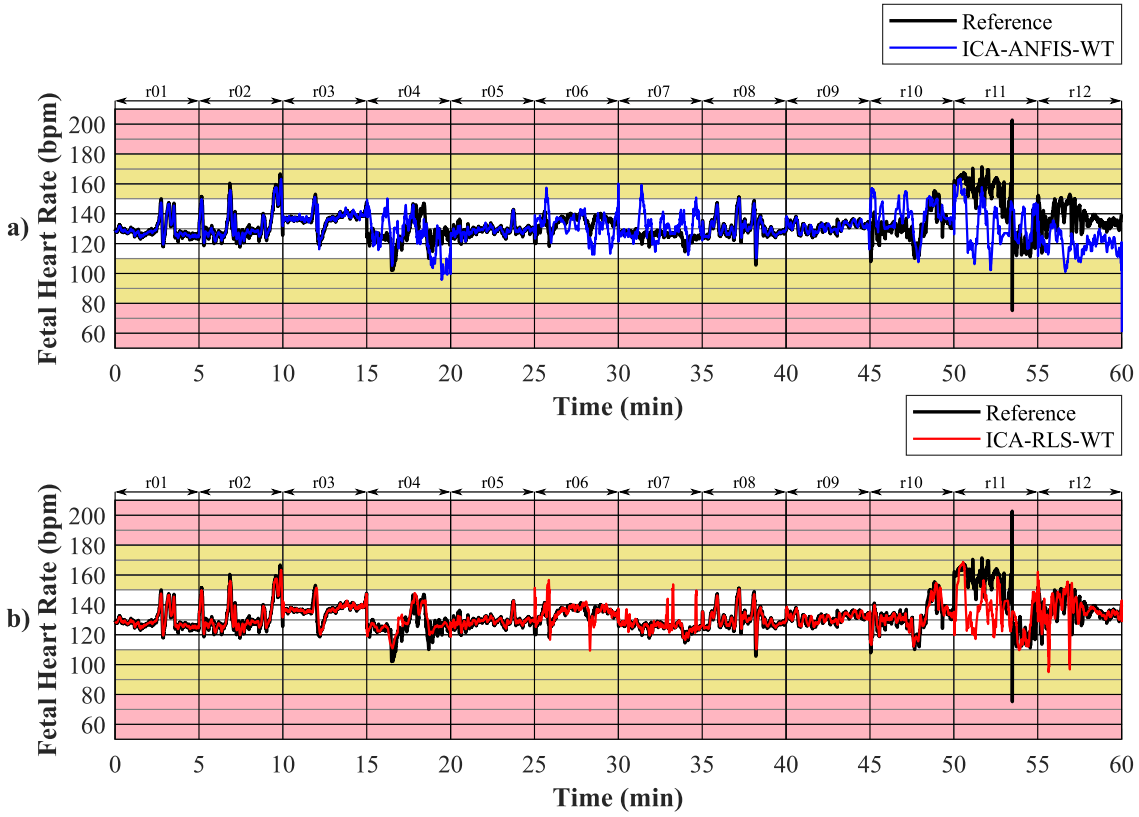

FIGURE 12. Graphical comparison of estimated and reference fHR variables over time from ADFECGDB database. a) comparison of estimated variables using the ICA-ANFIS-WT hybrid method; and b) comparison of estimated variables using the hybrid ICA-RLS-WT method.

surgical termination of pregnancy. Fig. 12 shows that the ICA-RLS-WT hybrid method provides more similar fHR variable curves over time than the ICA-ANFIS-WT hybrid method. Thus, it can be stated that, based on visual assessment, the ICA-RLS-WT hybrid method achieves better fECG signal extraction accuracy.

C. BLAND-ALTMAN GRAPHS

In this part of the test, Bland-Altman graphs were plotted between the individual estimated and reference fHR variables were over time after adjustments from chapter IV-B. Fig. 13 and 14 show 2 examples of accurate estimated variables of fHR over time and Fig. 15 and 16 show 2 examples of inaccurately estimated variables of fHR over time.

Initially, before the Bland-Altman graphs were plotted, two vectors were calculated between the individual estimated fHR variables over time and between the fHR reference variables over time using both hybrid methods. The first difference vectors $\overrightarrow{D}$ were made for the Y-axes, which show the dif-

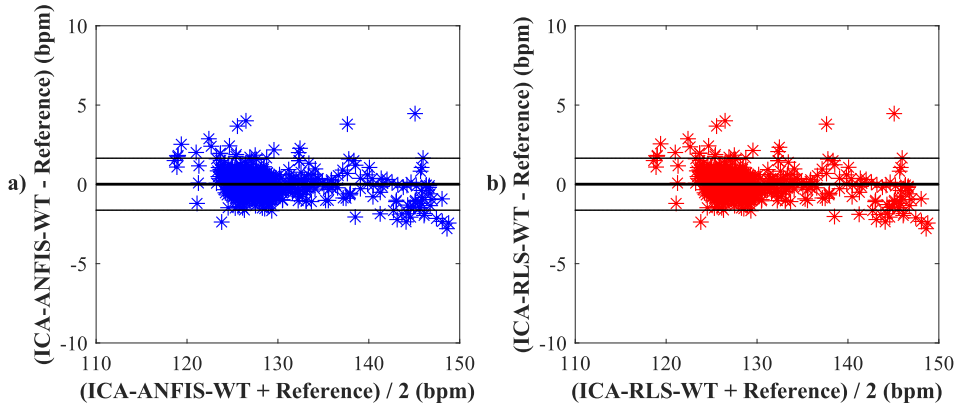

FIGURE 13. Comparison of estimated and reference variables of fHR over time from recording r01. a) comparison of the reference and estimated variables of fHR over time using ICA-ANFIS-WT based on the Bland-Altman graph; and b) comparison of the reference and estimated variables of fHR over time using ICA-RLS-WT based on the Bland-Altman graph.

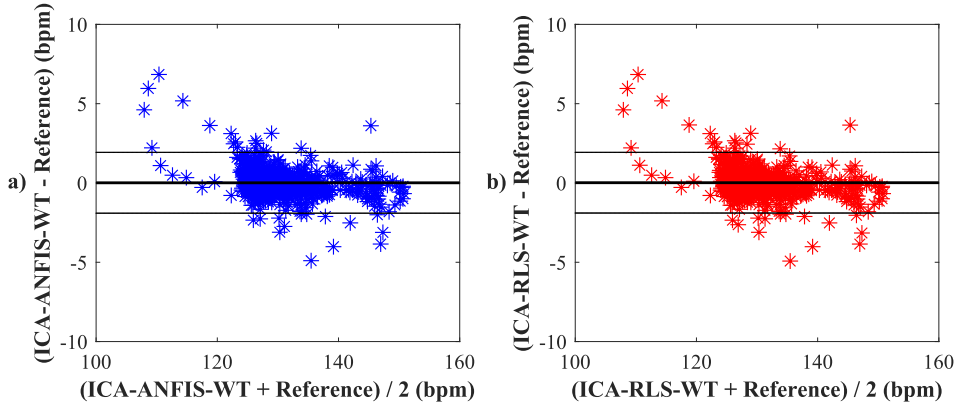

FIGURE 14. Comparison of estimated and reference variables of fHR over time from recording r08. a) comparison of the reference and estimated variables of fHR over time using ICA-ANFIS-WT based on the Bland-Altman graph; and b) comparison of the reference and estimated variables of fHR over time using ICA-RLS-WT based on the Bland-Altman graph.

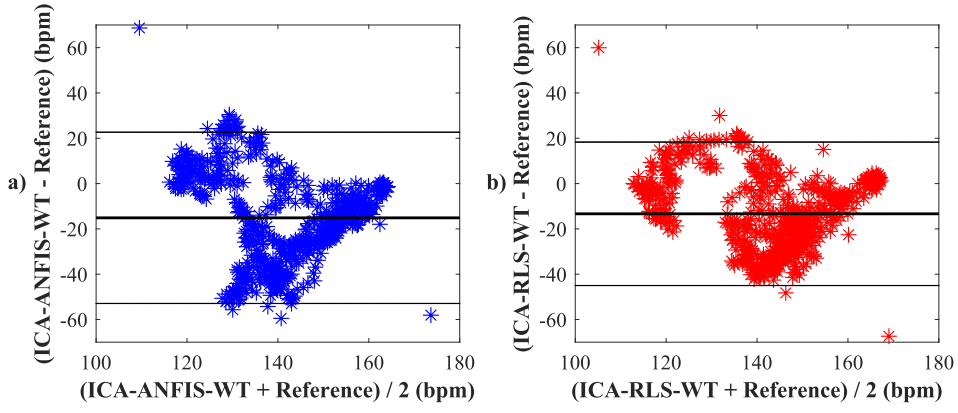

FIGURE 15. Comparison of estimated and reference variables of fHR over time from recording r11. a) comparison of the reference and estimated variables of fHR over time using ICA-ANFIS-WT based on the Bland-Altman graph; and b) comparison of the reference and estimated variables of fHR over time using ICA-RLS-WT based on the Bland-Altman graph.

ferences between the values of the fHR variables at the time of the reference and estimated signals, see equation (32). The second vectors $\overrightarrow{M}$ were made for the X-axes, which show the averages between the values of the fHR variables at the time of the reference and estimated signals, see equation (33). The elements of both of the vectors $\overrightarrow{D}$ and $\overrightarrow{M}$

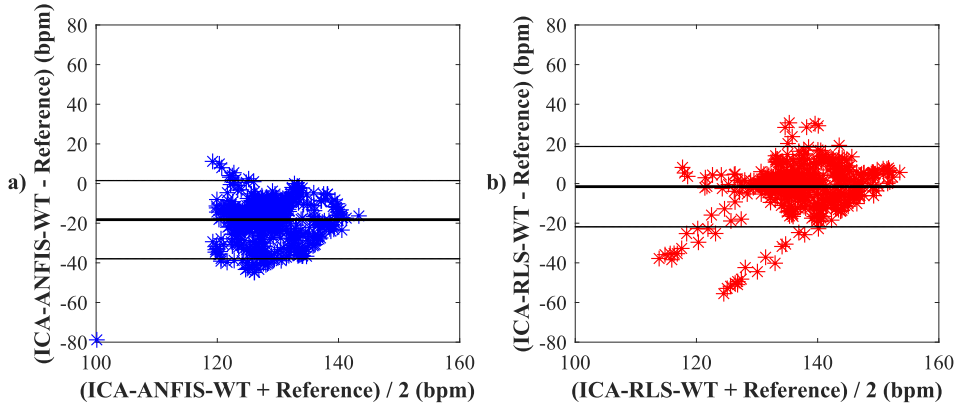

FIGURE 16. Comparison of estimated and reference variables of fHR over time from recording r12. a) comparison of the reference and estimated variables of fHR over time using ICA-ANFIS-WT based on the Bland-Altman graph; and b) comparison of the reference and estimated variables of fHR over time using ICA-RLS-WT based on the Bland-Altman graph.

were then plotted into individual Bland-Altman graphs. The main part of the Bland-Altman graph construction is the calculation of mean value μ, which is shown in the graph by the middle thick horizontal line. Subsequently, on the basis of this mean value μ and the calculated standard deviation σ, two LoAs are determined using $\mu \pm 1.96\sigma$ which are represented by the remaining two thinner lines in the graph. Equations (37), (38) and (39) are used for the calculation.

The individual mean values μ and values 1.96σ determined were recorded in Table 5. In the tables, it is necessary to monitor whether the mean value μ approaches 0. At a high positive or negative value, the mean value μ will show that there were large values in the difference vector $\overrightarrow{D}$ and, therefore, there is a large difference between the estimated and the reference variables of fHR over time. A similar phenomenon can be then observed in values 1.96σ. Table 5 shows that a low mean value μ was achieved for r01, r02, r03, r05, r08, and r09 recordings, indicating that the ICA-ANFIS-WT hybrid method is effective in these recordings. Nevertheless, r03 recording shows a fairly high value of 1.96σ, so, for this recording, we have to disprove the statement. This means that good fECG signal extraction efficiency using the hybrid ICA-ANFIS-WT method can be monitored, based on this testing, only in r01, r02, r05 r08 and r09 recordings.

Table 5 also shows that the ICA-RLS-WT hybrid method has low mean values μ for r01, r02, r03, r05, r06, r08, r09 and r10 recordings, indicating good efficiency of the ICA-RLS-WT hybrid method in these recordings. From the recordings marked, large value of 1.96σ can be seen in r03, r06 and 10 recordings, which means that good fECG signal extraction efficiency using the hybrid ICA-RLS-WT method can be monitored in the remaining 5 recordings.

D. ECG PHYSIONET CHALLENGE 2013

This chapter deals with evaluation of both hybrid methods on dataset from set A, Physionet Challenge 2013. Previous experiments proved that ICA-RLS-WT hybrid method performs better than ICA-ANFIS-WT hybrid method. Experiments carried out using ADFECGDB database were very extensive, so experiment carried out using Physionet Challenge 2013 database is performed only on evaluation of R-Peak detection accuracy (similar to experiment in chapter IV-A). After performing optimization and associated extractions on all 25 recordings using both hybrid methods, the detection of R-peaks was performer using a CWT-based detector. Then determination of of TP, FP and FN and calculation of selected parameters, ACC, SE, PPV and F1, was performed on all recording from Physionet Challenge 2013 database.

Table 6 shows the results for the ICA-ANFIS-WT hybrid method. It can be seen that the method worked, based on ACC, above 95 % with 6 recordings (a04, a05, a08, a15, a17 and a22), and over 80 % for a01 recording. On the basis of PPV, it worked, moreover, above 95 % with a01 recording, which, according to the ACC, SE and F1 parameters, did not reach 95 % accuracy. This fact indicates that, in the signal extracted, on a01 recording, there was a low number

TABLE 5. The recorded mean values and values after plotting Bland-Altman graph for individual adjusted and estimated fHR variables over time using the ICA-ANFIS-WT and ICA-RLS-WT hybrid methods relative to fHR reference variables over time.

Recording	(ICA-ANFIS-WT)		(ICA-RLS-WT)	
	μ (bpm)	1.96σ (bpm)	μ (bpm)	1.96σ (bpm)
r01	0.01	1.64	0.01	1.64
r02	0.03	3.00	0.03	3.06
r03	0.46	5.15	0.12	5.31
r04	-1.94	25.63	1.28	8.84
r05	-0.02	2.38	0.01	1.91
r06	-2.08	15.84	0.27	10.40
r07	5.25	17.43	0.99	8.34
r08	0.01	1.92	0.02	1.91
r09	-0.15	4.28	-0.08	4.19
r10	6.12	19.31	0.11	7.81
r11	-15.12	37.79	-13.34	31.65
r12	-18.21	19.72	-1.56	20.25

TABLE 6. Determination of TP, FP and FN based on the detection of R-peak locations in the fECG signals extracted from Physionet Challenge 2013 database using the hybrid ICA-ANFIS-WT method relative to R-peak locations in the reference signal, and calculation of the ACC, SE, PPV and F1 parameters.

Recording	Combination of electrodes	Shape of membership functions	Number of membership functions	Number of epochs	Number of R-peaks by annotations	TP	FP	FN	ACC (%)	SE (%)	PPV (%)	F1 (%)
a01	1,3,4	gaussmf	2	10	145	131	3	14	88.51	90.35	97.76	93.91
a02	1,3	trimf	8	20	160	33	94	127	12.99	20.63	25.98	23.00
a03	3,4	gaussmf	2	10	128	74	30	54	46.84	57.81	71.15	63.79
a04	1,2	gaussmf	2	10	129	129	0	0	100	100	100	100
a05	1,4	gaussmf	2	10	129	129	0	0	100	100	100	100
a06	2,4	gbellmf	6	30	160	101	29	59	53.44	63.13	77.69	69.66
a07	1,2,3,4	trapmf	2	10	130	81	58	49	43.09	62.31	58.27	60.22
a08	1,4	gaussmf	2	10	128	128	0	0	100	100	100	100
a09	1,3,4	trapmf	6	20	130	27	68	103	13.64	20.77	28.42	24.00
a10	1,2,3,4	gaussmf	8	10	175	139	12	36	74.33	79.43	92.05	85.28
a11	1,3,4	trimf	10	30	140	31	72	109	14.62	22.14	30.10	25.51
a12	3,4	gaussmf	10	30	138	68	7	70	46.90	49.28	90.67	63.85
a13	1,2,4	trimf	2	30	126	98	29	28	63.23	77.78	77.17	77.47
a14	2,3	trapmf	2	30	123	63	37	60	39.38	51.22	63.00	56.50
a15	1,4	gaussmf	2	10	134	134	0	0	100	100	100	100
a16	1,3,4	trapmf	10	30	130	28	63	102	14.51	21.54	30.77	25.34
a17	1,2,4	trimf	4	30	132	132	0	0	100	100	100	100
a18	1,3,4	trapmf	4	30	150	25	89	125	10.46	16.67	21.93	18.94
a19	1,2,4	trimf	2	30	127	100	26	27	65.36	78.74	79.37	79.05
a20	1,2,3	trimf	6	20	131	62	65	69	31.63	47.33	48.82	48.06
a21	1,3,4	gaussmf	2	30	145	109	14	36	68.55	75.17	88.62	81.34
a22	1,4	gaussmf	2	10	126	126	0	0	100	100	100	100.00
a23	2,3,4	trimf	2	30	126	107	23	19	71.81	84.92	82.31	83.59
a24	2,3,4	trimf	2	30	123	95	28	28	62.91	77.24	77.24	77.24
a25	2,3,4	trimf	2	20	125	101	29	24	65.58	80.80	77.69	79.22

TABLE 7. Determination of TP, FP and FN based on the detection of R-peak locations in the fECG signals extracted from Physionet Challenge 2013 database using the hybrid ICA-RLS-WT method relative to R-peak locations in the reference signal, and calculation of the ACC, SE, PPV and F1 parameters.

Recording	Combination of electrodes	Filter order	Number of R-peaks by annotations	TP	FP	FN	ACC (%)	SE (%)	PPV (%)	F1 (%)
a01	1,3,4	10	145	126	7	19	82.90	86.90	94.74	90.65
a02	1,2,4	2	160	31	90	129	12.40	19.38	25.62	22.06
a03	1,4	100	128	126	2	2	96.92	98.44	98.44	98.44
a04	1,2	64	129	129	0	0	100	100	100	100
a05	1,3	32	129	126	0	3	97.67	97.67	100	98.82
a06	2,4	24	160	95	39	65	47.74	59.38	70.90	64.63
a07	1,2,3,4	66	130	71	68	59	35.86	54.62	51.08	52.79
a08	1,4	100	128	128	0	0	100	100	100	100
a09	1,4	94	130	24	36	106	14.46	18.46	40.00	25.26
a10	2,4	98	175	119	14	56	62.96	68.00	89.47	77.27
a11	1,4	24	140	29	23	111	17.79	20.71	55.77	30.21
a12	1,3,4	14	138	130	2	8	92.86	94.20	98.49	96.30
a13	2,4	36	126	107	13	19	76.98	84.92	89.17	86.99
a14	1,2,3,4	10	123	116	11	7	86.57	94.31	91.34	92.80
a15	1,4	94	134	134	0	0	100	100	100	100
a16	1,4	40	130	21	22	109	13.82	16.15	48.84	24.28
a17	1,4	100	132	132	0	0	100	100	100	100
a18	1,2,3,4	34	150	18	56	132	8.74	12.00	24.32	16.07
a19	3,4	42	127	115	4	12	87.79	90.55	96.64	93.50
a20	1,4	96	131	70	2	61	52.63	53.44	97.22	68.97
a21	2,3,4	4	145	108	20	37	65.46	74.48	84.38	79.12
a22	1,4	32	126	126	0	0	100	100	100	100
a23	1,3	36	126	104	16	22	73.24	82.54	86.67	84.55
a24	1,3	50	123	117	3	6	92.86	95.12	97.50	96.30
a25	2,3	94	125	117	10	8	86.67	93.60	92.13	92.86

of FP values, but a high number of FN values. With the other recordings, this method did not achieve good results, and, thus, it was not, as an extraction method, effective in these recordings.

The same assessment was performed for the hybrid ICA-RLS-WT method and the results can be seen in Table 7. Based on the ACC parameter, this method achieved values above 95 % with 7 recordings (a03, a04, a05, a08, a15, a17 and

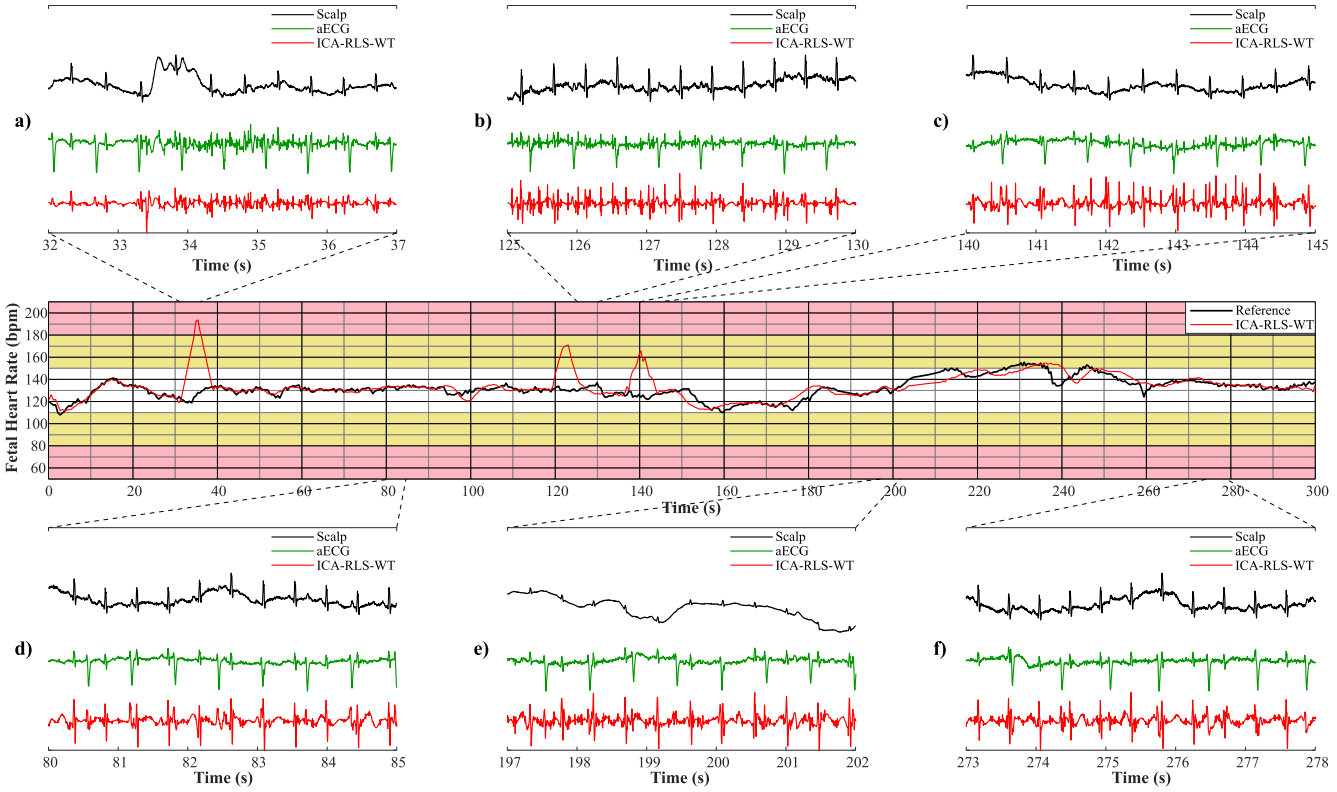

FIGURE 17. Estimated fHR variable curve over time using the ICA-RLS-WT hybrid method on r10 recording. Graphs a), b) and c) show 3 selected sections where filtration did not work, and graphs d), e) and f) show 3 selected sections where filtration worked properly.

a22), values over 90 % for a12 and a24 recordings, and over 80 % for a01, a14, a19 and a25 recordings. With the signal extracted from a12 recording, the method, based on the PPV and F1 parameters, reached a values above 95 %. This fact indicates that, in the signal extracted, on a12 recording, there was a low number of FP values, but a high number of FN values. With the signal extracted from a24 recording, the method, based on the SE, PPV and F1 parameters, reached a values above 95 %. With the signal extracted from a19 recording, the method, based on PPV, reached a value above 95 %. This fact indicates that, in the signal extracted, on a19 recording, there was a low number of FP values, but a high number of FN values. With the other 12 recordings out of 25, the ICA-RLS-WT hybrid method was not effective.

During this experiment, the ICA-RLS-WT hybrid method achieved significantly better results than the ICA-ANFIS-WT hybrid method. It can be seen that, in 9 recordings out of 25, the ICA-RLS-WT hybrid method was able to extract fECG signals that reached at least 90 % based on the ACC parameter, and, as a result, with 13 recordings out of 25, they reached at least 80 % based on the ACC parameter. The ICA-ANFIS-WT hybrid method was able to extract usable fECG signals in only 7 recordings out of 25.

V. CONCLUSION AND DISCUSSION

The results summarized in the previous subchapters show that the algorithms presented are very effective for most of the recordings tested. However, for some recordings or their sections, their effectiveness is limited. As an example, recording r10 will be discussed in detail in this chapter in connection with the ICA-RLS-WT method.

Fig. 17 shows the estimated fHR variable curve using the given method and in comparison with the reference fHR curve obtained from FSE recording. Further, this figure contains six selected 5 s sections, three of which relate to cases where the resulting fHR curve deviated significantly from the reference and, in case of longer duration, this could lead to a false positive diagnosis of fetal distress. The remaining three sections then relate to cases where the specified fHR matches the reference. The analysis of these six sections includes an example of three signals from a given time interval: the reference signal from the FSE, abdominal electrode 1, and, also, the signal estimated using the ICA-RLS-WT method. It is clear from these examples that the quality of the extraction depends on the quality of the input abdominal signals. In the case of sections where the recording quality was inadequate, i.e. a) to c), this algorithm was not able to suppress this interference, which resulted in an increase in the number of false positive peaks (FP), thus reducing the parameters evaluating extraction quality (ACC, PPV, F1). With sections d) - f) having good-quality abdominal recordings, the useless signal was suppressed to such an extent that successful detection of fetal R waves was possible; therefore, the fHR curve determined is consistent with the reference. Hence,

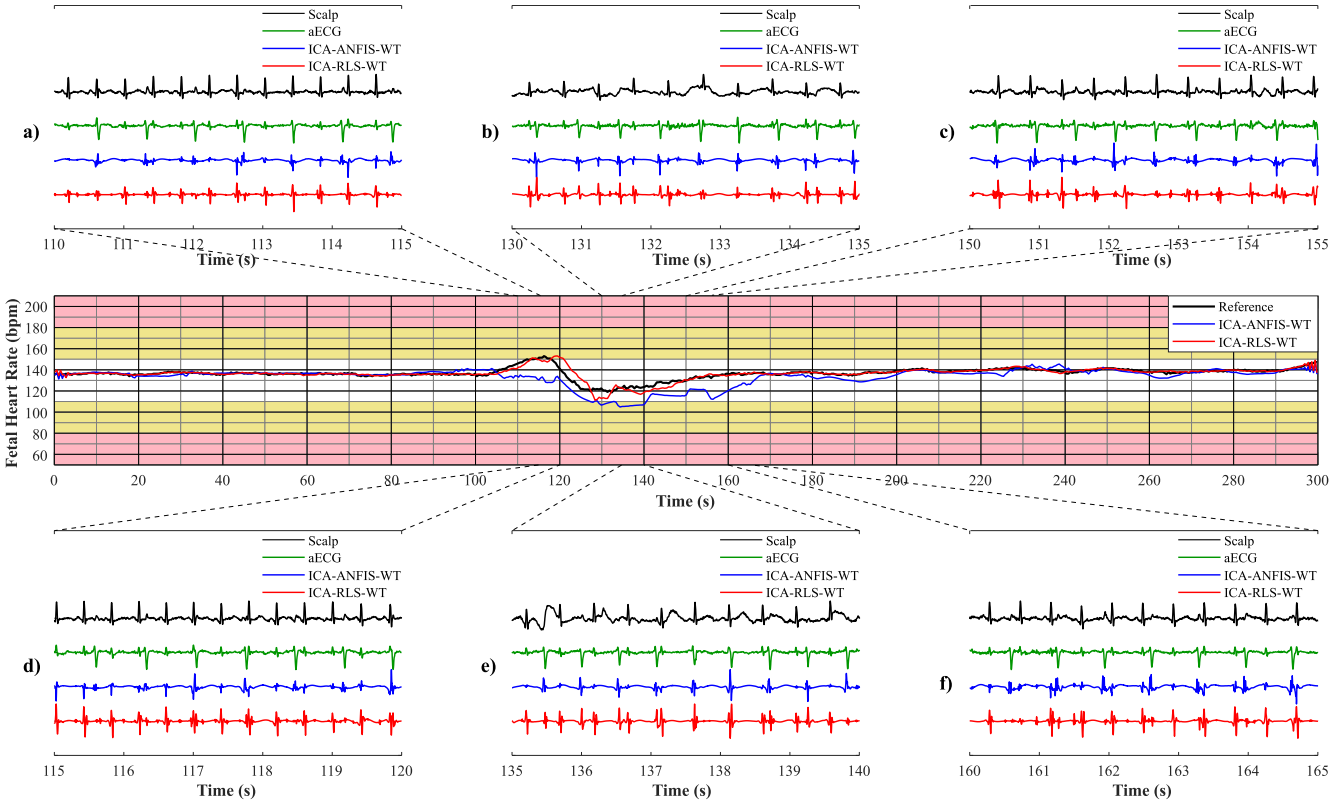

FIGURE 18. Estimated fHR variable curve over time using the ICA-ANFIS-WT and ICA-RLS-WT hybrid methods on r03 recording. Graphs a) to f) show selected sections for a comparison of the efficiency of both methods.

in the case of clinical use of this method, it is essential to maintain a high quality of the abdominal recording. It is negatively influenced in particular by insufficient adhesion of the measuring electrodes and their placement, fetal position and maternal movement.

Another factor that has a tremendous impact on the quality of extraction using the hybrid system presented here is the optimal adjustment of adaptive algorithms. As examined in [71], this setting varies depending on the placement of the input electrodes (reference thoracic and abdominal ones). In this case, however, the reference maternal signal is estimated using AES methods. Therefore, in further research, a more detailed study of optimizing the adaptive algorithm settings is required, particularly depending on various factors, such as the selection of the quantity and location of the hybrid system input electrodes, the gestational age of the fetus or its position. At the same time, it is necessary to test and compare combinations of different algorithms in each block of the hybrid extraction system depending on the factors mentioned above.

Fig. 18 shows a comparison of fHR variable curves determined using the ICA-ANFIS-WT and ICA-RLS-WT methods tested in r03 recording compared to the reference fHR curve obtained from the FSE recording. It can be stated that the ICA-RLS-WT method is more capable of copying the trend within the resulting fHR curve. The method using ANFIS was not able to suppress the maternal component from the abdominal recording in some sections, and the resulting fHR thus correlated with the maternal heart rate that is lower than fetal one. On the other hand, the method using the RLS algorithm, with some exceptions as section e), was able to successfully suppress the maternal component to such an extent that it did not affect the subsequent detection of R-R intervals, hence the calculation of the resulting fHR.

Fig. 19 shows the example of the reference output signal and the fHR waveforms along with those estimated by means of hybrid methods ICA-ANFIS-WT and ICA-RLS-WT on a08 recording, where the filtrations achieved 100 % for all the evaluation parameters. The fHR determined using the estimated fECG signal is almost identical with the reference fHR signal.

Fig. 20 shows the example of the reference output signal and the fHR waveforms along with those estimated by means of hybrid methods ICA-ANFIS-WT and ICA-RLS-WT on a18 recording, i.e. the recording with the worst results. It can be noticed that in the input aECG signal, the magnitude of the fetal component is negligible in comparison with the maternal one. For such signal, the extraction is challenging.

It should be noted that the Physionet Challenge 2013 dataset is composed of variety of data. Part of the data was taken from various fECG databases using various electrode deployment, while some were synthetic. It can

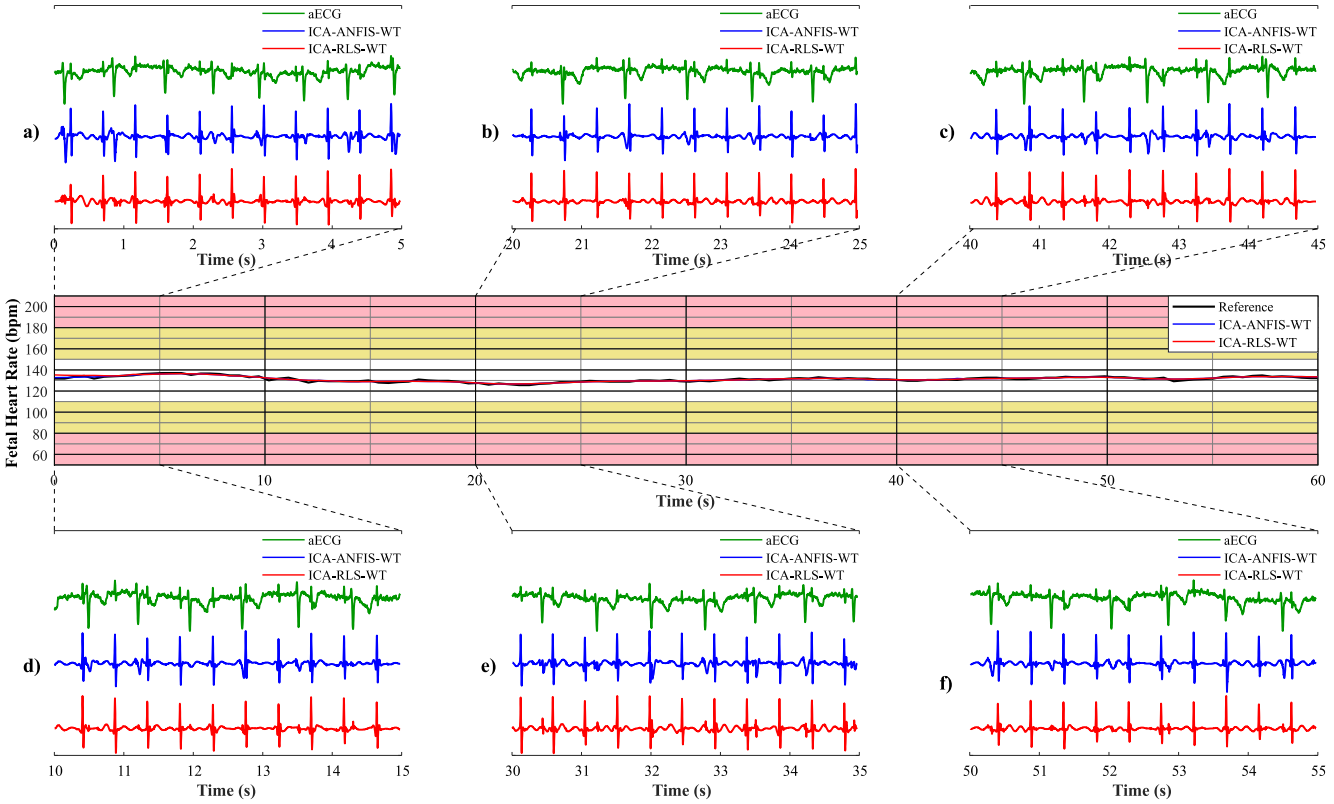

FIGURE 19. Estimated fHR variable curve over time using the ICA-ANFIS-WT and ICA-RLS-WT hybrid methods on a08 recording. Graphs a)–f) show selected sections in recording where filtration worked properly.

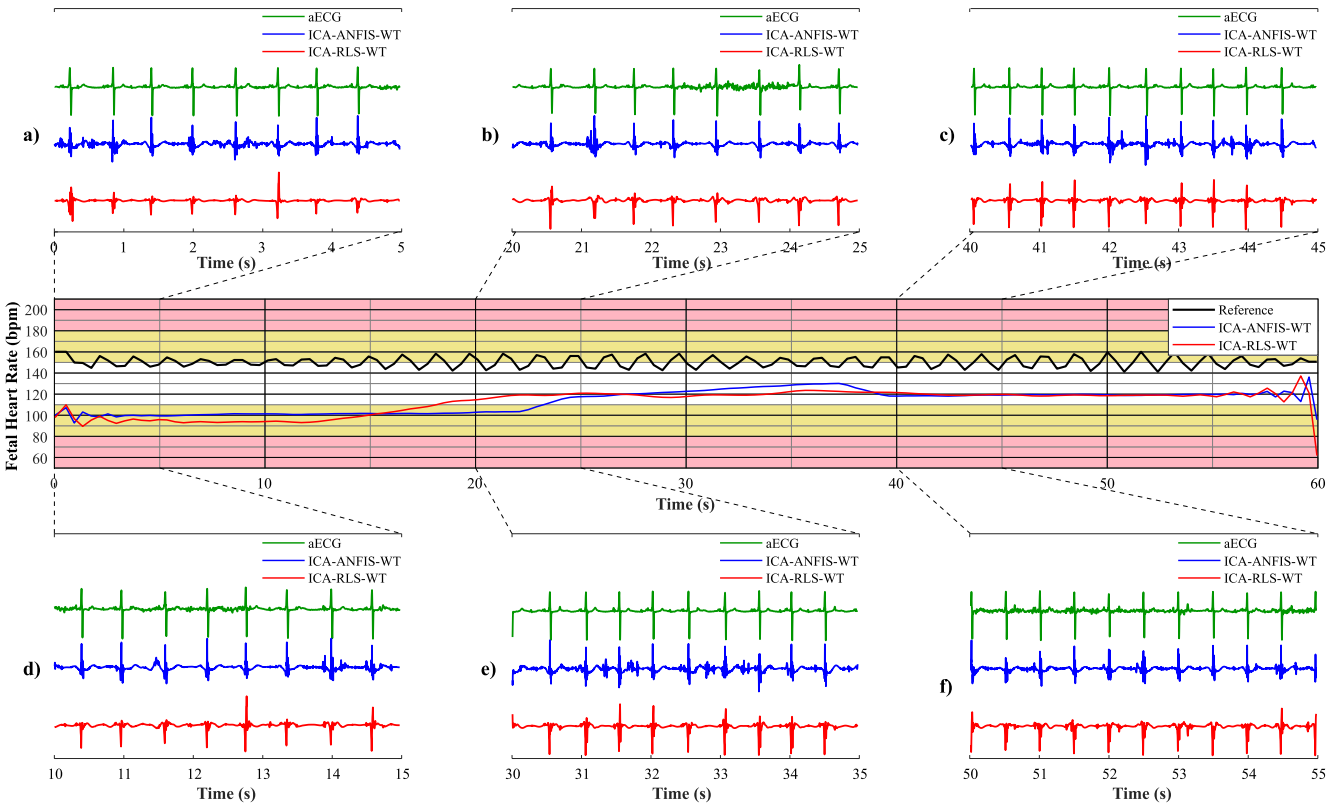

FIGURE 20. Estimated fHR variable curve over time using the ICA-ANFIS-WT and ICA-RLS-WT hybrid methods on a18 recording. Graphs a)–f) show selected sections in recording where filtration did not work.

be noticed that the signals significantly differ from the real recordings that were used in the rest of the experiments in the time domain and also in terms of the determined fHR.

Hybrid methods combine the benefits of both adaptive and non-adaptive approaches, such as accuracy, stability, and minimization of the number of measuring electrodes. This study shows that this approach is very promising for the extraction of fECG and very accurate for the needs of determining fHR as the main parameter observed in current clinical practice. The subject of further research should be deeper morphological analysis, such as ST segment, QT interval or T/QRS ratio analysis. This would lead to the creation of a new diagnostic method - a non-invasive variant of STAN, i.e. NI-STAN, thus improving diagnosis of fetal hypoxia.

In this work, wavelet transform was used in the last step. This method is very effective for the purpose of detecting R-peaks, which is important for determining the heart rate. On the other hand, this method has negative effects on the ECG curve morphology. Therefore, for the purposes of NI-STAN, a replacement for the final post-processing step would have to be found in this hybrid system in the future. Nevertheless, it can be stated that the construction of hybrid methods achieves promising efficiency in fECG signal extraction, hence, it can be assumed that these methods could be used in clinical practice as a replacement for classical CTG. However, before introducing this method into clinical practice, the negative factors affecting the efficiency of the extraction system need to be addressed. They include, in particular, the quality of abdominal recordings, which is primarily influenced by the location and adhesion of the measuring electrodes, and the maternal or fetal movement.

In this initial study, particular attention was paid to the precise determination of fHR. However, in clinical practice, both fHR and uterine contractions are monitored by CTG during electronic fetal monitoring. In the case of an ECG-based system, the electrical signal produced by the contracting uterus could be recorded by a method known as electrohysterography (EHG), whose efficacy has been verified in e.g. [137]–[140]. For future research, it is necessary to incorporate measurement and filtration of uterine contractions into a complex NI-fECG-based fetal monitoring system.

The proposed hybrid system could be improved by modifying its individual parts. The adaptive algorithms could be upgraded or replaced by different adaptive methods. For example, in the future research, we aim to test LMS, normalized LMS, QR-RLS, or adaptive linear neuron (ADALINE). Most of these algorithms are part of MATLAB digital signal processing toolbox. The advantage of using an adaptive algorithm as a major part of a hybrid system is that it compensates delays and the inference.

Another part that can be modified is the initial block of the extraction system for estimation of the mECG input to the adaptive algorithm. The currently used ICA algorithm could be replaced by another method able to estimate the maternal component, such as the PCA algorithm. The advantage of using the ICA algorithm (or PCA algorithm) is that it only requires abdominal electrodes as an input (the chest electrodes are not needed).

In terms of the WT algorithm, it is necessary to mention that its utilization influences the morphology of the ECG waveform and thus disables the morphological analysis. So, in our future research we will only use WT algorithm to find correct R-peak positions (for fHR monitoring) while the morphological analysis will be performed only on the signals that were not processed by the WT algorithm.

The approach introduced in this paper is only an example of possible hybrid fECG extraction systems. There is a large variety of the hybrid systems among the literature [97]. Most of the currently available hybrid methods utilize the ICA algorithm. Very interesting hybrid methods are for example combination of ICA, ensemble empirical mode decomposition (EEMD) and wavelet shrinkage (WS) [98], combination of ICA and adaptive fECG enhancer (AFE) [99], combination of ICA and projective filtering (PF) [100], combination of ICA and PCA [101], combination of singular value decomposition (SVD) and ICA [102], etc. In our future research, we aim to test some of the most promising methods and modify our system according to the results.

ETHICS STATEMENT

The study protocol was approved by the Ethical Committee of the Silesian Medical University, Katowice, Poland (NN-013-345/02). Subjects read the approved consent form and gave written informed consent to participate in the study.

REFERENCES

[1] C. Sureau, "Historical perspectives: Forgotten past, unpredictable future," *Baillière's Clin. Obstetrics Gynaecol.*, vol. 10, no. 2, pp. 167–184, 1996. doi: 10.1016/S0950-3552(96)80032-0.

[2] H. D. Banta and S. B. Thacker, "Historical controversy in health technology assessment: The case of electronic fetal monitoring," *Obstetrical Gynecol. Survey*, vol. 56, no. 11, pp. 707–719, 2001. doi: 10.1097/00006254-200111000-00023.

[3] C. B. Martin, Jr., "Electronic fetal monitoring: A brief summary of its development, problems and prospects," *Eur. J. Obstetrics Gynecol. Reproductive Biol.*, vol. 78, no. 2, pp. 133–140, 1998. doi: 10.1016/S0301-2115(98)00059-1.

[4] C. A. Menihan and E. Kopel, *Electronic Fetal Monitoring: Concepts and Applications*. Philadelphia, PA, USA: Lippincott Williams & Wilkins, 2007.

[5] V. A. Browne, C. G. Julian, L. Toledo-Jaldin, D. Cioffi-Ragan, E. Vargas, and L. G. Moore, "Uterine artery blood flow, fetal hypoxia and fetal growth," *Philos. Trans. Roy. Soc., Biol. Sci.*, vol. 370, no. 1663, 2015, Art. no. 20140068. doi: 10.1098/rstb.2014.0068.

[6] H. Y. Chen, S. P. Chauhan, C. V. Ananth, A. M. Vintzileos, and A. Z. Abuhamad, "Electronic fetal heart rate monitoring and its relationship to neonatal and infant mortality in the United States," *Amer. J. Obstetrics Gynecol.*, vol. 204, no. 6, pp. 491.e1–491.e10, 2011. doi: 10.1016/j.ajog.2011.04.024.

[7] Z. Alfirevic, D. Devane, G. M. Gyte, and A. Cuthbert, "Continuous cardiotocography (CTG) as a form of electronic fetal monitoring (EFM) for fetal assessment during labour," *Cochrane Database Syst. Rev.*, no. 2, pp. 1–137, Feb. 2017, Art. no. CD006066. doi: 10.1002/14651858.CD006066.pub3.

[8] J. Jezewski, J. Wrobel, and K. Horoba, "Comparison of Doppler ultrasound and direct electrocardiography acquisition techniques for quantification of fetal heart rate variability," *IEEE Trans. Biomed. Eng.*, vol. 53, no. 5, pp. 855–864, May 2006. doi: 10.1109/TBME.2005.863945.

[9] M. F. MacDorman and E. C. W. Gregory, "Fetal and perinatal mortality: United States, 2013," *Nat. Vital Statist. Rep.*, vol. 64, no. 8, pp. 1–24, 2015.

[10] H. D. Banta and S. B. Thacker, "Costs and benefits of electronic fetal monitoring: A review of the literature," US Dept. Health, Educ., Welfare, Public Health Service, Office Health Res., Statist., Technol., Nat. Center Health Services Res., Hyattsville, MD, USA, ERIC no. ED171429, 1979.
[11] P. J. Placek, "Type of delivery associated with social, demographic, maternal health, infant health and health insurance factors," Nat. Center Health Statist., Hyattsville, MD, USA, Tech. Rep., 1972, pp. 619–624.
[12] R. H. Paul, J. R. Huey, Jr., and C. F. Yaeger, "Clinical fetal monitoring: Its effect on cesarean section rate and perinatal mortality: Five-year trends," *Postgraduate Med.*, vol. 61, no. 4, pp. 160–166, 1977. doi: 10.1080/00325481.1977.11714552.
[13] D. Petitti, R. O. Olson, and R. L. Williams, "Cesarean section in California—1960 through 1975," *Amer. J. Obstetrics Gynecol.*, vol. 133, no. 4, pp. 391–397, 1979. doi: 10.1016/0002-9378(79)90058-9.
[14] R. L. Williams and W. E. Hawes, "Cesarean section, fetal monitoring, and perinatal mortality in California," *Amer. J. Public Health*, vol. 69, no. 9, pp. 864–870, 1979. doi: 10.2105/AJPH.69.9.864.
[15] S. M. Taffel, P. J. Placek, M. Moien, and C. L. Kosary, "1989 U.S. Cesarean section rate steadies—VBAC rate rises to nearly one in five," *Birth*, vol. 18, no. 2, pp. 73–77, 1991. doi: 10.1111/j.1523-536X.1991.tb00063.x.
[16] S. B. Thacker, D. F. Stroup, and H. B. Peterson, "Efficacy and safety of intrapartum electronic fetal monitoring: An update," *Obstetrics Gynecol.*, vol. 86, no. 4, pp. 613–620, 1995. doi: 10.1016/S0029-7844(95)80027-1.
[17] E. L. Ryding, K. Wijma, and B. Wijma, "Psychological impact of emergency cesarean section in comparison with elective cesarean section, instrumental and normal vaginal delivery," *J. Psychosomatic Obstetrics Gynecol.*, vol. 19, no. 3, pp. 135–144, 1998. doi: 10.3109/01674829809025691.
[18] E. L. Ryding, B. Wijma, and K. Wijma, "Posttraumatic stress reactions after emergency cesarean section," *Acta Obstetricia Gynecologica Scandinavica*, vol. 76, no. 9, pp. 856–861, 1997. doi: 10.3109/00016349709024365.
[19] J. E. Swain, E. Tasgin, L. C. Mayes, R. Feldman, R. Todd, and J. F. Leckman, "Maternal brain response to own baby-cry is affected by cesarean section delivery," *J. Child Psychol. Psychiatry*, vol. 49, no. 10, pp. 1042–1052, 2008. doi: 10.1111/j.1469-7610.2008.01963.x.
[20] S. Petrou, J. Henderson, and C. Glazener, "Economic aspects of caesarean section and alternative modes of delivery," *Best Pract. Res. Clin. Obstetrics Gynaecology*, vol. 15, no. 1, pp. 145–163, 2001. doi: 10.1053/beog.2000.0154.
[21] J. Henderson, R. McCandlish, L. Kumiega, and S. Petrou, "Systematic review of economic aspects of alternative modes of delivery," *Int. J. Obstetrics Gynaecol.*, vol. 108, no. 2, pp. 149–157, 2001.
[22] M. Cremer, "Ueber die direkte ableitung der aktionsstrome des menschlichen herzens vom oesophagus und uber das elektrokardiogramm des fotus," *Miinchener Medizinische Wochenschrift*, vol. 53, no. 17, pp. 811–813, 1906.
[23] C. Sureau and R. Foulon, "Etude de l'activite electrique de l'uterus au cours de la gestation et du travail. . .," Tech. Rep., 1955.
[24] S. D. Larks, "Fetal electrocardiography. The electrical activity of the fetal heart," *Amer. J. Med. Sci.*, vol. 242, no. 3, p. 395, 1961.
[25] C. Sureau and R. Trocellier, "Un problème technique d'électrocardiographie foetale. Note sur l'élimination de l'électrocardiogramme maternel," *Gynecology Obstetrics*, vol. 60, no. 1, pp. 43–54, 1961.
[26] J. B. Roche and E. H. Hon, "The fetal electrocardiogram: V. Comparison of lead systems," *Amer. J. Obstetrics Gynecol.*, vol. 92, no. 8, pp. 1149–1159, 1965. doi: 10.1016/S0002-9378(15)33099-4.
[27] S. Zaunseder, F. Andreotti, M. Cruz, H. Stepan, C. Schmieder, H. Malberg, and N. Wessel, "Fetal QRS detection by means of Kalman filtering and using the event synchronous canceller," in *Proc. 7th Int. Workshop Biosig. Interpretation*, Como, Italy, Jul. 2012, pp. 2–4.
[28] L. D. Lathauwer, B. D. Moor, and J. Vandewalle, "Fetal electrocardiogram extraction by blind source subspace separation," *IEEE Trans. Biomed. Eng.*, vol. 47, no. 5, pp. 567–572, May 2000. doi: 10.1109/10.841326.
[29] R. Sameni, C. Jutten, and M. B. Shamsollahi, "What ICA provides for ECG processing: Application to noninvasive fetal ECG extraction," in *Proc. IEEE Int. Symp. Signal Process. Inf. Technol.*, Vancouver, BC, Canada, Aug. 2006, pp. 656–661. doi: 10.1109/ISSPIT.2006.270882.
[30] M. Richter, T. Schreiber, and D. T. Kaplan, "Fetal ECG extraction with nonlinear state-space projections," *IEEE Trans. Biomed. Eng.*, vol. 45, no. 1, pp. 133–137, Jan. 1998. doi: 10.1109/10.650369.
[31] M. Kotas, J. Jezewski, T. Kupka, and K. Horoba, "Detection of low amplitude fetal QRS complexes," in *Proc. 30th Annu. Int. Conf. IEEE Eng. Med. Biol. Soc.*, Vancouver, BC, Canada, Aug. 2008, pp. 4764–4767. doi: 10.1109/IEMBS.2008.4650278.
[32] J. Behar, J. Oster, and G. D. Clifford, "Combining and benchmarking methods of foetal ECG extraction without maternal or scalp electrode data," *Physiol. Meas.*, vol. 35, no. 8, p. 1569, 2014. doi: 10.1088/0967-3334/35/8/1569.
[33] S. M. M. Martens, C. Rabotti, M. Mischi, and R. J. Sluijter, "A robust fetal ECG detection method for abdominal recordings," *Physiol. Meas.*, vol. 28, no. 4, pp. 373–388, 2007. doi: 10.1088/0967-3334/28/4/004.
[34] P. P. Kanjilal, S. Palit, and G. Saha, "Fetal ECG extraction from single-channel maternal ECG using singular value decomposition," *IEEE Trans. Biomed. Eng.*, vol. 44, no. 1, pp. 51–59, Jan. 1997. doi: 10.1109/10.553712.
[35] J. Behar, "Extraction of clinical information from the non-invasive fetal electrocardiogram," (2016), *arXiv:1606.01093*. [Online]. Available: https://arxiv.org/abs/1606.01093
[36] R. Vullings, B. de Vries, and J. W. M. Bergmans, "An adaptive Kalman filter for ECG signal enhancement," *IEEE Trans. Biomed Eng.*, vol. 58, no. 4, pp. 1094–1103, Apr. 2011. doi: 10.1109/TBME.2010.2099229.
[37] G. Bachmann, L. Narici, and E. Beckenstein, *Fourier and Wavelet Analysis*. New York, NY, USA: Springer-Verlag, 2012.
[38] S. H. Jothi and K. H. Prabha, "Fetal electrocardiogram extraction using adaptive neuro-fuzzy inference systems and undecimated wavelet transform," *IETE J. Res.*, vol. 58, no. 6, pp. 469–475, 2012. doi: 10.4103/0377-2063.106753.
[39] H. Hassanpour and A. Parsaei, "Fetal ECG extraction using wavelet transform," in *Proc. Int. Conf. Comput. Intell. Modelling Control Automat. Intell. Agents Web Technol. Int. Commerce (CIMCA)*, Sydney, NSW, Australia, Nov./Dec. 2006, p. 179. doi: 10.1109/CIMCA.2006.98.
[40] P. Kumar, S. K. Sharma, and S. Prasad, "CAD for detection of fetal electrocardiogram by using wavelets and neuro-fuzzy systems," *Int. J. Appl. Eng. Res.*, vol. 11, no. 4, pp. 2321–2326, 2016.
[41] K. Assaleh and H. Al-Nashash, "A novel technique for the extraction of fetal ECG using polynomial networks," *IEEE Trans. Biomed. Eng.*, vol. 52, no. 6, pp. 1148–1152, Jun. 2005. doi: 10.1109/TBME.2005.844046.
[42] S. Kadambe, R. Murray, and G. F. Boudreaux-Bartels, "Wavelet transform-based QRS complex detector," *IEEE Trans. Biomed. Eng.*, vol. 46, no. 7, pp. 838–848, Jul. 1999. doi: 10.1109/10.771194.
[43] R. Almeida, H. Gonçalves, J. Bernardes, and A. P. Rocha, "Fetal QRS detection and heart rate estimation: A wavelet-based approach," *Physiol. Meas.*, vol. 35, no. 8, pp. 1723–1735, 2014. doi: 10.1088/0967-3334/35/8/1723.
[44] M. G. Jafari and J. A. Chambers, "Fetal electrocardiogram extraction by sequential source separation in the wavelet domain," *IEEE Trans. Biomed. Eng.*, vol. 52, no. 3, pp. 390–400, Mar. 2005. doi: 10.1109/TBME.2004.842958.
[45] E. Castillo, D. P. Morales, G. Botella, A. García, L. Parrilla, and A. J. Palma, "Efficient wavelet-based ECG processing for single-lead FHR extraction," *Digit. Signal Process.*, vol. 23, no. 6, pp. 1897–1909, 2013. doi: 10.1016/j.dsp.2013.07.010.
[46] S. A. Chouakri, F. Bereksi-Reguig, S. Ahmaldi, and O. Fokapu, "Wavelet denoising of the electrocardiogram signal based on the corrupted noise estimation," in *Proc. Comput. Cardiol.*, Lyon, France, Sep. 2005, pp. 1021–1024. doi: 10.1109/CIC.2005.1588284.
[47] C. H. L. Peters, R. Vullings, M. J. Rooijakkers, J. W. M. Bergmans, S. G. Oei, and P. F. F. Wijn, "A continuous wavelet transform-based method for time-frequency analysis of artefact-corrected heart rate variability data," *Physiol. Meas.*, vol. 32, no. 10, pp. 1517–1527, 2011. doi: 10.1088/0967-3334/32/10/001.
[48] A. Khamene and S. Negahdaripour, "A new method for the extraction of fetal ECG from the composite abdominal signal," *IEEE Trans. Biomed. Eng.*, vol. 47, no. 4, pp. 507–516, Apr. 2000. doi: 10.1109/10.828150.
[49] F. Mochimaru, Y. Fujimoto, and Y. Ishikawa, "Detecting the fetal electrocardiogram by wavelet theory-based methods," *Prog. Biomed. Res.*, vol. 7, pp. 185–193, Sep. 2002.
[50] E. C. Karvounis, C. Papaloukas, D. I. Fotiadis, and L. K. Michalis, "Fetal heart rate extraction from composite maternal ECG using complex continuous wavelet transform," in *Proc. Comput. Cardiol.*, Chicago, IL, USA, Sep. 2004, pp. 737–740. doi: 10.1109/CIC.2004.1443044.

[51] B. Azzerboni, F. La Foresta, N. Mammone, and F. C. Morabito, "A new approach based on wavelet-ICA algorithms for fetal electrocardiogram extraction," in *Proc. ESANN*, Bruges, Belgium, Apr. 2005, pp. 193–198.
[52] S. Wu, Y. Shen, Z. Zhou, L. Lin, Y. Zeng, and X. Gao, "Research of fetal ECG extraction using wavelet analysis and adaptive filtering," *Comput. Biol. Med.*, vol. 43, no. 10, pp. 1622–1627, 2013.
[53] A. Daamouche, L. Hamami, N. Alajlan, and F. Melgani, "A wavelet optimization approach for ECG signal classification," *Biomed. Signal Process. Control*, vol. 7, no. 4, pp. 342–349, Jul. 2012. doi: 10.1016/j.bspc.2011.07.001.
[54] V. S. Chourasia and A. K. Mittra, "Selection of mother wavelet and denoising algorithm for analysis of foetal phonocardiographic signals," *J. Med. Eng. Technol.*, vol. 33, no. 6, pp. 442–448, 2009. doi: 10.1080/03091900902952618.
[55] R. Martinek, R. Kahankova, J. Nedoma, M. Fajkus, and K. Cholevova, "Fetal ECG preprocessing using wavelet transform," in *Proc. 10th Int. Conf. Comput. Modeling Simulation*, 2018, pp. 39–43.
[56] S. Ravindrakumar and K. B. Raja, "Fetal ECG extraction and enhancement in prenatal monitoring—Review and implementation issues," in *Proc. Trendz Inf. Sci. Comput. (TISC)*, Chennai, India, Dec. 2010, pp. 16–20. doi: 10.1109/TISC.2010.5714599.
[57] V. Zarzoso and A. K. Nandi, "Noninvasive fetal electrocardiogram extraction: Blind separation versus adaptive noise cancellation," *IEEE Trans. Biomed. Eng.*, vol. 48, no. 1, pp. 12–18, Jan. 2001. doi: 10.1109/10.900244.
[58] R. Martinek, R. Kahankova, J. Jezewski, R. Jaros, J. Mohylova, M. Fajkus, J. Nedoma, P. Janku, and H. Nazeran, "Comparative effectiveness of ICA and PCA in extraction of fetal ECG from abdominal signals: Toward non-invasive fetal monitoring," *Frontiers Physiol.*, vol. 9, p. 648, May 2018. doi: 10.3389/fphys.2018.00648.
[59] R. Sameni, C. Jutten, and M. B. Shamsollahi, "Multichannel electrocardiogram decomposition using periodic component analysis," *IEEE Trans. Biomed. Eng.*, vol. 55, no. 8, pp. 1935–1940, Aug. 2008. doi: 10.1109/TBME.2008.919714.
[60] S. Kharabian, M. B. Shamsollahi, and R. Sameni, "Fetal R-wave detection from multichannel abdominal ECG recordings in low SNR," in *Proc. Annu. Int. Conf. IEEE Eng. Med. Biol. Soc.*, Minneapolis, MN, USA, Sep. 2009, pp. 344–347. doi: 10.1109/IEMBS.2009.5333578.
[61] J. L. Camargo-Olivares, R. Martin-Clemente, S. Hornillo-Mellado, M. M. Elena, and I. Roman, "The maternal abdominal ECG as input to MICA in the fetal ECG extraction problem," *IEEE Signal Process. Lett.*, vol. 18, no. 3, pp. 161–164, Mar. 2011. doi: 10.1109/LSP.2011.2104415.
[62] Y. Sevim and A. Atasoy, "Performance evaluation of nonparametric ICA algorithm for fetal ECG extraction," *Turkish J. Elect. Eng. Comput. Sci.*, vol. 19, no. 4, pp. 657–666, 2011. doi: 10.3906/elk-0912-311.
[63] D. E. Marossero, D. Erdogmus, N. Euliano, J. C. Principe, and K. E. Hild, "Independent components analysis for fetal electrocardiogram extraction: A case for the data efficient mermaid algorithm," in *Proc. IEEE 13th Workshop Neural Netw. Signal Process.*, Toulouse, France, Sep. 2003, pp. 399–408. doi: 10.1109/NNSP.2003.1318039.
[64] Y. Ye, Z.-L. Zhang, J. Zeng, and L. Peng, "A fast and adaptive ICA algorithm with its application to fetal electrocardiogram extraction," *Appl. Math. Comput.*, vol. 205, no. 2, pp. 799–806, 2008. doi: 10.1016/j.amc.2008.05.117.
[65] V. Zarzoso, A. K. Nandi, and E. Bacharakis, "Maternal and foetal ECG separation using blind source separation methods," *Math. Med. Biol., J. IMA*, vol. 14, no. 3, pp. 207–225, Sep. 1997. doi: 10.1093/imammb/14.3.207.
[66] R. Swarnalatha and D. V. Prasad, "A novel technique for extraction of FECG using multi stage adaptive filtering," *J. Appl. Sci.*, vol. 10, no. 4, pp. 319–324, 2010.
[67] R. Kahankova, J. Jezewski, J. Nedoma, M. Jezewski, M. Fajkus, A. Kawala-Janik, H. Wen, and R. Martinek, "Influence of gestation age on the performance of adaptive systems for fetal ECG extraction," *Adv. Electr. Electron. Eng.*, vol. 15, no. 3, pp. 491–501, 2017. doi: 10.15598/aeee.v15i3.2207.
[68] G. Camps, M. Martinez, and E. Soria, "Fetal ECG extraction using an FIR neural network," in *Proc. Comput. Cardiol.*, Rotterdam, The Netherlands, vol. 28, Sep. 2001, pp. 249–252. doi: 10.1109/CIC.2001.977639.
[69] R. Kahankova, R. Martinek, and P. Bilik, "Non-invasive fetal ECG extraction from maternal abdominal ECG using LMS and RLS adaptive algorithms," in *Proc. Int. Afro-Eur. Conf. Ind. Adv.*, Marrakesh, Morrocco, Nov. 2016, pp. 258–271. doi: 10.1007/978-3-319-60834-1_27.
[70] R. Martinek and J. Žídek, "Refining the diagnostic quality of the abdominal fetal electrocardiogram using the techniques of artificial intelligence," VSB–Tech. Univ. Ostrava, Ostrava, Czech Republic, Tech. Rep., 2012.
[71] R. Martinek, R. Kahankova, H. Nazeran, J. Konecny, J. Jezewski, P. Janku, P. Bilik, J. Zidek, J. Nedoma, and M. Fajkus, "Non-invasive fetal monitoring: A maternal surface ECG electrode placement-based novel approach for optimization of adaptive filter control parameters using the LMS and RLS algorithms," *Sensors*, vol. 17, no. 5, p. 1154, 2017. doi: 10.3390/s17051154.
[72] M. B. I. Reaz and L. S. Wei, "Adaptive linear neural network filter for fetal ECG extraction," in *Proc. Int. Conf. Intell. Sens. Inf. Process.*, Chennai, India, Jan. 2004, pp. 321–324. doi: 10.1109/ICISIP.2004.1287675.
[73] W. Jia, C. Yang, G. Zhong, M. Zhou, and S. Wu, "Fetal ECG extraction based on adaptive linear neural network," in *Proc. 3rd Int. Conf. Biomed. Eng. Informat.*, Yantai, China, vol. 2, Oct. 2010, pp. 899–902. doi: 10.1109/BMEI.2010.5639886.
[74] M. A. Hasan, M. I. Ibrahimy, and M. B. I. Reaz, "Fetal ECG extraction from maternal abdominal ECG using neural network," *J. Softw. Eng. Appl.*, vol. 2, no. 5, p. 330, 2009.
[75] R. Kahankova, R. Martinek, M. Mikolášová, and R. Jaroš, "Adaptive linear neuron for fetal electrocardiogram extraction," in *Proc. IEEE 20th Int. Conf. e-Health Netw., Appl. Services (Healthcom)*, Ostrava, Czech Republic, Sep. 2018, pp. 1–5. doi: 10.1109/HealthCom.2018.8531135.
[76] W. Zheng, H. Liu, A. He, X. Ning, and J. Cheng, "Single-lead fetal electrocardiogram estimation by means of combining R-peak detection, resampling and comb filter," *Med. Eng. Phys.*, vol. 32, no. 7, pp. 708–719, 2010. doi: 10.1016/j.medengphy.2010.04.012.
[77] Z. Wei, W. Xueyun, Z. J. jian, and L. Hongxing, "Noninvasive fetal ECG estimation using adaptive comb filter," *Comput. Methods Programs Biomed.*, vol. 112, no. 1, pp. 125–134, 2013. doi: 10.1016/j.cmpb.2013.07.015.
[78] M. Shadaydeh, Y. Xiao, and R. K. Ward, "Extraction of fetal ECG using adaptive volterra filters," in *Proc. 16th Eur. Signal Process. Conf.*, Lausanne, Switzerland, Aug. 2008, pp. 1–5.
[79] P. Wang and S. Tan, "Soft computing and fuzzy logic," *Soft Comput.*, vol. 1, no. 1, pp. 35–41, 1997. doi: 10.1007/s005000050004.
[80] M. Nasiri, K. Faez, and A. M. Nasrabadi, "A new method for extraction of fetal electrocardiogram signal based on adaptive nero-fuzzy inference system," in *Proc. IEEE Int. Conf. Signal Image Process. Appl. (ICSIPA)*, Kuala Lumpur, Malaysia, Nov. 2011, pp. 456–461. doi: 10.1109/ICSIPA.2011.6144151.
[81] A. Sargolzaei, K. Faez, and S. Sargolzaei, "A new method for foetal electrocardiogram extraction using adaptive nero-fuzzy interference system trained with PSO algorithm," in *Proc. IEEE Int. Conf. Electro/Inf. Technol.*, Mankato, MN, USA, May 2011, pp. 1–5. doi: 10.1109/EIT.2011.5978624.
[82] S. S. Priyadharsini, S. E. Rajan, and S. Saranya, "An efficient soft-computing technique for extracting fetal ECG from maternal ECG signal," *Program. Device Circuits Syst.*, vol. 3, no. 1, pp. 1–7, 2011.
[83] S. R. Rathod and V. R. Bansod, "Separation of FECG from complex ECG in fetal monitoring," in *Proc. Online Int. Conf. Green Eng. Technol. (IC-GET)*, Coimbatore, India, Nov. 2016, pp. 1–5. doi: 10.1109/GET.2016.7916788.
[84] R. Swarnalatha and D. V. Prasad, "Maternal ECG cancellation in abdominal signal using ANFIS and wavelets," *Appl Sci.*, vol. 10, pp. 868–877, Nov. 2010.
[85] H. Ahmadieh and B. M. Asl, "Fetal ECG extraction via type-2 adaptive neuro-fuzzy inference systems," *Comput. Methods Programs Biomed.*, vol. 142, pp. 101–108, Apr. 2017. doi: 10.1016/j.cmpb.2017.02.009.
[86] P. Kumar, S. K. Sharma, and S. Prasad, "Detection of fetal electrocardiogram through OFDM, neuro-fuzzy logic and wavelets systems for telemetry," in *Proc. 10th Int. Conf. Intell. Syst. Control (ISCO)*, Coimbatore, India, Jan. 2016, pp. 1–4. doi: 10.1109/ISCO.2016.7726970.
[87] K. Assaleh, "Extraction of fetal electrocardiogram using adaptive neuro-fuzzy inference systems," *IEEE Trans. Biomed. Eng.*, vol. 54, no. 1, pp. 59–68, Jan. 2007. doi: 10.1109/TBME.2006.883728.
[88] R. Martinek, H. Skutova, R. Kahankova, P. Koudelka, P. Bilik, and J. Koziorek, "Fetal ECG extraction based on adaptive neuro-fuzzy interference system," in *Proc. 10th Int. Symp. Commun. Syst., Netw. Digit. Signal Process. (CSNDSP)*, Prague, Czech Republic, Jul. 2016, pp. 1–6. doi: 10.1109/CSNDSP.2016.7573973.
[89] J. Behar, A. Johnson, G. D. Clifford, and J. Oster, "A comparison of single channel fetal ECG extraction methods," *Ann. Biomed. Eng.*, vol. 42, no. 6, pp. 1340–1353, 2014. doi: 10.1007/s10439-014-0993-9.

[90] G. Clifford, R. Sameni, J. Ward, J. Robinson, and A. J. Wolfberg, "Clinically accurate fetal ECG parameters acquired from maternal abdominal sensors," *Amer. J. Obstetrics Gynecol.*, vol. 205, no. 1, pp. 47.e1–47.e5, 2011. doi: 10.1016/j.ajog.2011.02.066.

[91] J. Behar, T. Zhu, J. Oster, A. Niksch, D. Y. Mah, T. Chun, J. Greenberg, C. Tanner, J. Harrop, R. Sameni, J. Ward, A. J. Wolfberg, and G. D. Clifford, "Evaluation of the fetal QT interval using non-invasive fetal ECG technology," *Physiol. Meas.*, vol. 37, no. 9, pp. 1392–1403, 2016. doi: 10.1088/0967-3334/37/9/1392.

[92] *Monica Healthcare*. Accessed: Aug. 7, 2019. [Online]. Available: http://www.monicahealthcare.com/

[93] *Mindchild*. Accessed: Aug. 7, 2019. [Online]. Available: http://www.mindchild.com/

[94] M. A. Belfort *et al.*, "A randomized trial of intrapartum fetal ECG ST-segment analysis," *New England J. Med.*, vol. 373, no. 7, pp. 632–641, 2015. doi: 10.1056/NEJMoa1500600.

[95] I. Amer-Wåhlin, C. Hellsten, H. Norén, H. Hagberg, A. Herbst, I. Kjellmer, H. Lilja, C. Lindoff, M. Månsson, L. Mårtensson, P. Olofsson, A.-K. Sundström, and K. Maršál, "Cardiotocography only versus cardiotocography plus ST analysis of fetal electrocardiogram for intrapartum fetal monitoring: A Swedish randomised controlled trial," *Lancet*, vol. 358, no. 9281, pp. 534–538, 2001. doi: 10.1016/S0140-6736(01)05703-8.

[96] M. G. Ross, L. D. Devoe, and K. G. Rosen, "ST-segment analysis of the fetal electrocardiogram improves fetal heart rate tracing interpretation and clinical decision making," *J. Maternal-Fetal Neonatal Med.*, vol. 15, no. 3, pp. 181–185, 2004. doi: 10.1080/14767050410001668284.

[97] R. Jaros, R. Martinek, and R. Kahankova, "Non-adaptive methods for fetal ECG signal processing: A review and appraisal," *Sensors*, vol. 18, no. 11, p. 3648, 2018. doi: 10.3390/s18113648.

[98] G. Liu and Y. Luan, "An adaptive integrated algorithm for noninvasive fetal ECG separation and noise reduction based on ICA-EEMD-WS," *Med. Biol. Eng. Comput.*, vol. 53, no. 11, pp. 1113–1127, 2015. doi: 10.1007/s11517-015-1389-1.

[99] A. Gupta, M. C. Srivastava, V. Khandelwal, and A. Gupta, "A novel approach to fetal ECG extraction and enhancement using blind source separation (BSS-ICA) and adaptive fetal ECG enhancer (AFE)," in *Proc. 6th Int. Conf. Inf., Commun. Signal Process.*, Singapore, Dec. 2007, pp. 1–4. doi: 10.1109/ICICS.2007.4449716.

[100] M. Kotas, "Combined application of independent component analysis and projective filtering to fetal ECG extraction," *Biocybern. Biomed. Eng.*, vol. 28, no. 1, p. 75, 2008.

[101] R. Martín-Clemente, J. L. Camargo-Olivares, S. Hornillo-Mellado, M. Elena, and I. Roman, "Fast technique for noninvasive fetal ECG extraction," *IEEE Trans. Biomed. Eng.*, vol. 58, no. 2, pp. 227–230, Feb. 2011. doi: 10.1109/TBME.2010.2059703.

[102] P. Gao, E.-C. Chang, and L. Wyse, "Blind separation of fetal ECG from single mixture using SVD and ICA," in *Proc. 4th Joint Int. Conf. Inf., Commun. Signal Process., 4th Pacific Rim Conf. Multimedia*, Singapore, vol. 3, Dec. 2003, pp. 1418–1422. doi: 10.1109/ICICS.2003.1292699.

[103] *Neoventa: It's All in the Beat*. Accessed: Aug. 7, 2019. [Online]. Available: https://www.neoventa.com/products/stan/

[104] J. Jezewski, A. Matonia, T. Kupka, D. Roj, and R. Czabanski, "Determination of fetal heart rate from abdominal signals: Evaluation of beat-to-beat accuracy in relation to the direct fetal electrocardiogram," *Biomedizinische Technik/Biomed. Eng.*, vol. 57, no. 5, pp. 383–394, 2012. doi: 10.1515/bmt-2011-0130.

[105] M. Kotas, J. Jezewski, A. Matonia, and T. Kupka, "Towards noise immune detection of fetal QRS complexes," *Comput. Methods Programs Biomed.*, vol. 97, no. 3, pp. 241–256, 2010. doi: 10.1016/j.cmpb.2009.09.005.

[106] Q. Yu, H. Yan, L. Song, W. Guo, H. Liu, J. Si, and Y. Zhao, "Automatic identifying of maternal ECG source when applying ICA in fetal ECG extraction," *Biocybern. Biomed. Eng.*, vol. 38, no. 3, pp. 448–455, 2018. doi: 10.1016/j.bbe.2018.03.003.

[107] L. D. Sharma, R. Asery, R. K. Sunkaria, and D. Mittal, "Comparative study of fetal ECG elicitation using adaptive filtering techniques," in *Proc. 2nd Int. Conf. Adv. Elect., Electron., Inf., Commun. Bio-Inform. (AEEICB)*, Chennai, India, Feb. 2016, pp. 68–72. doi: 10.1109/AEEICB.2016.7538399.

[108] P. Sutha and V. E. Jayanthi, "Fetal electrocardiogram extraction and analysis using adaptive noise cancellation and wavelet transformation techniques," *J. Med. Syst.*, vol. 42, no. 1, p. 21, 2018. doi: 10.1007/s10916-017-0868-3.

[109] D. J. Jagannath and A. I. Selvakumar, "Issues and research on foetal electrocardiogram signal elicitation," *Biomed. Signal Process. Control*, vol. 10, pp. 224–244, Mar. 2014. doi: 10.1016/j.bspc.2013.11.001.

[110] R. Kahankova, R. Jaros, R. Martinek, J. Jezewski, H. Wen, M. Jezewski, and A. Kawala-Janik, "Non-adaptive methods of fetal ECG signal processing," *Adv. Elect. Electron. Eng.*, vol. 15, no. 3, pp. 476–490, 2017. doi: 10.15598/aeee.v15i3.2196.

[111] D. Luo, "Research and application of fetal electrocardiogram blind signal separation technology," *Res. J. Appl. Sci. Eng. Technol.*, vol. 4, no. 14, pp. 2231–2235, 2012.

[112] A. Hyvärinen and E. Oja, "Independent component analysis: Algorithms and applications," *Neural Netw.*, vol. 13, nos. 4–5, pp. 411–430, Jun. 2000. doi: 10.1016/S0893-6080(00)00026-5.

[113] R. Martinek, J. Zidek, P. Bilik, J. Manas, J. Koziorek, Z. Teng, and H. Wen, "The use of LMS and RLS adaptive algorithms for an adaptive control method of active power filter," *Energy Power Eng.*, vol. 5, no. 4, pp. 1126–1133, 2013. doi: 10.4236/epe.2013.54B215.

[114] R. Kahankova, R. Martinek, and P. Bilik, "Fetal ECG extraction from abdominal ECG using RLS based adaptive algorithms," in *Proc. 18th Int. Carpathian Control Conf. (ICCC)*, Sinaia, Romania, May 2017, pp. 337–342. doi: 10.1109/CarpathianCC.2017.7970422.

[115] J.-S. R. Jang, "ANFIS: Adaptive-network-based fuzzy inference system," *IEEE Trans. Syst., Man, Cybern.*, vol. 23, no. 3, pp. 665–685, May/Jun. 1993. doi: 10.1109/21.256541.

[116] M. Pokorny and Z. Krisova, "Knowledge systems," Moravian Bus. College Olomouc, Olomouc, Czech Republic, Tech. Rep., 2016.

[117] K. Tanaka and H. O. Wang, *Fuzzy Control Systems Design and Analysis: A Linear Matrix Inequality Approach*. Hoboken, NJ, USA: Wiley, 2004.

[118] B. Widrow and M. A. Lehr, "30 years of adaptive neural networks: Perceptron, Madaline, and backpropagation," *Proc. IEEE*, vol. 78, no. 9, pp. 1415–1442, Sep. 1990. doi: 10.1109/5.58323.

[119] P. J. Werbos, "Backpropagation through time: What it does and how to do it," *Proc. IEEE*, vol. 78, no. 10, pp. 1550–1560, Oct. 1990. doi: 10.1109/5.58337.

[120] K. Assaleh, "Adaptive neuro-fuzzy inference systems for extracting fetal electrocardiogram," in *Proc. IEEE Int. Symp. Signal Process. Inf. Technol.*, Vancouver, BC, Canada, Aug. 2006, pp. 122–126. doi: 10.1109/ISSPIT.2006.270782.

[121] R. Bhoker and J. P. Gawande, "Fetal ECG extraction using wavelet transform," *ITSI Trans. Elect. Electron. Eng*, vol. 1, pp. 2320–8945, 2013.

[122] V. S. Chourasia and A. K. Tiwari, "Design methodology of a new wavelet basis function for fetal phonocardiographic signals," *Sci. World J.*, vol. 2013, Apr. 2013, Art. no. 505840. doi: 10.1155/2013/505840.

[123] D. Valencia, D. Orejuela, J. Salazar, and J. Valencia, "Comparison analysis between rigrsure, sqtwolog, heursure and minimaxi techniques using hard and soft thresholding methods," in *Proc. 21st Symp. Signal Process., Images Artif. Vis. (STSIVA)*, Bucaramanga, Colombia, Aug./Sep. 2016, pp. 1–5. doi: 10.1109/STSIVA.2016.7743309.

[124] C. Taswell, "The what, how, and why of wavelet shrinkage denoising," *Computing Sci. Eng.*, vol. 2, no. 3, pp. 12–19, May 2000. doi: 10.1109/5992.841791.

[125] L. Billeci and M. Varanini, "A combined independent source separation and quality index optimization method for fetal ECG extraction from abdominal maternal leads," *Sensors*, vol. 17, no. 5, p. 1135, 2017. doi: 10.3390/s17051135.

[126] M. Litschmannova, "Introduction to statistics," Fac. Elect. Eng. Comput. Sci., VSB-Tech. Univ. Ostrava, Ostrava, Czech Republic, Tech. Rep., 2011.

[127] J. M. Bland and D. G. Altman, "Measuring agreement in method comparison studies," *Stat. Methods Med. Res.*, vol. 8, no. 2, pp. 135–160, Jun. 1999. doi: 10.1177/096228029900800204.

[128] M. Fajkus, J. Nedoma, R. Martinek, V. Vasinek, H. Nazeran, and P. Siska, "A non-invasive multichannel hybrid fiber-optic sensor system for vital sign monitoring," *Sensors*, vol. 17, no. 1, p. 111, Jan. 2017. doi: 10.3390/s17010111.

[129] A. Matonia, J. Jezewski, T. Kupka, K. Horoba, J. Wrobel, and A. Gacek, "The influence of coincidence of fetal and maternal QRS complexes on fetal heart rate reliability," *Med. Biol. Eng. Comput.*, vol. 44, no. 5, pp. 393–403, 2006. doi: 10.1007/s11517-006-0054-0.

[130] M. Kotas, J. Jezewski, K. Horoba, and A. Matonia, "Application of spatio-temporal filtering to fetal electrocardiogram enhancement," *Comput. Methods Programs Biomed.*, vol. 104, no. 1, pp. 1–9, 2011. doi: 10.1016/j.cmpb.2010.07.004.

[131] A. L. Goldberger, L. A. N. Amaral, L. Glass, J. M. Hausdorff, P. Ivanov, R. G. Mark, J. E. Mietus, G. B. Moody, C.-K. Peng, and H. E. Stanley, "PhysioBank, PhysioToolkit, and PhysioNet: Components of a new research resource for complex physiologic signals," *Circulation*, vol. 101, no. 23, pp. e215–e220, 2000. doi: 10.1161/01.CIR.101.23.e215.
[132] R. Sameni and G. D. Clifford, "A review of fetal ECG signal processing; Issues and promising directions," *Open Pacing, Electrophysiol. Therapy J.*, vol. 3, p. 4, Jan. 2010. doi: 10.2174/1876536X01003010004.
[133] C. Li, C. Zheng, and C. Tai, "Detection of ECG characteristic points using wavelet transforms," *IEEE Trans. Biomed. Eng.*, vol. 42, no. 1, pp. 21–28, Jan. 1995. doi: 10.1109/10.362922.
[134] A. Ghaffari, H. Golbayani, and M. Ghasemi, "A new mathematical based QRS detector using continuous wavelet transform," *Comput. Electr. Eng.*, vol. 34, no. 2, pp. 81–91, 2008. doi: 10.1016/j.compeleceng.2007.10.005.
[135] P. Du, W. A. Kibbe, and S. M. Lin, "Improved peak detection in mass spectrum by incorporating continuous wavelet transform-based pattern matching," *Bioinformatics*, vol. 22, no. 17, pp. 2059–2065, 2006. doi: 10.1093/bioinformatics/btl355.
[136] T. Kazmi, F. Radfer, and S. Khan, "ST Analysis of the fetal ECG, as an adjunct to fetal heart rate monitoring in labour: A review," *Oman Med. J.*, vol. 26, no. 6, pp. 459–460, 2011. doi: 10.5001/omj.2011.118.
[137] Y. Ye-Lin, J. Garcia-Casado, G. Prats-Boluda, J. Alberola-Rubio, and A. Perales, "Automatic identification of motion artifacts in EHG recording for robust analysis of uterine contractions," *Comput. Math. Methods Med.*, vol. 2014, Jan. 2014, Art. no. 470786.
[138] E. M. Graatsma, "Monitoring of fetal heart rate and uterine activity," Ph.D. dissertation, Dept. Perinatol. Gynaecol., Univ. Med. Center Utrecht, Utrecht, The Netherlands, 2010.
[139] B. C. Jacod, E. M. Graatsma, E. Van Hagen, and G. H. A. Visser, "A validation of electrohysterography for uterine activity monitoring during labour," *J. Maternal-Fetal Neonatal Med.*, vol. 23, no. 1, pp. 17–22, 2010. doi: 10.3109/14767050903156668.
[140] M. T. Garcia-Gonzalez, S. Charleston-Villalobos, C. Vargas-Garcia, R. Gonzalez-Camarena, and T. Aljama-Corrales, "Characterization of EHG contractions at term labor by nonlinear analysis," in *Proc. 35th Annu. Int. Conf. IEEE Eng. Med. Biol. Soc. (EMBC)*, Osaka, Japan, Jul. 2013, pp. 7432–7435. doi: 10.1109/EMBC.2013.6611276.

RENE JAROS was born in Ostrava, Czech Republic, in 1992. He graduated from the Faculty of Electrical Engineering and Computer Science, VSB—Technical University of Ostrava, in 2015. He is currently pursuing the Ph.D. degree in technical cybernetics with the VSB—Technical University of Ostrava. His bachelor thesis dealt with transformation methods of 12-lead electrocardiogram (ECG) to VCG, in 2015. His diploma thesis dealt with non-adaptive methods of fetal ECG signal processing, in 2017. His research interests include fetal electrocardiogram (fECG) extraction by using hybrid methods.

RADEK MARTINEK was born in Czech Republic, in 1984. He received the master's degree in information and communication technology from the VSB—Technical University of Ostrava, where he has been a Research Fellow, since 2012. In 2014, he successfully defended his dissertation thesis titled "The Use of Complex Adaptive Methods of Signal Processing for Refining the Diagnostic Quality of the Abdominal Fetal Electrocardiogram." In 2017, he became an Associate Professor in technical cybernetics after defending the habilitation thesis titled "Design and Optimization of Adaptive Systems for Applications of Technical Cybernetics and Biomedical Engineering Based on Virtual Instrumentation." He has been an Associate Professor with the VSB—Technical University of Ostrava, since 2017. His current research interests include digital signal processing (linear and adaptive filtering, soft computing-artificial intelligence and adaptive fuzzy systems, non-adaptive methods, biological signal processing, and digital processing of speech signals), wireless communications (software-defined radio), and power quality improvement. He has more than 200 journals and conference articles in his research areas.

RADANA KAHANKOVA was born in Opava, Czech Republic, in 1991. She received the bachelor's degree and the master's degree in biomedical engineering from the Department of Cybernetics and Biomedical Engineering, VSB—Technical University of Ostrava, in 2014 and 2016, respectively. She is currently pursuing the Ph.D. degree in technical cybernetics. Her current research interest includes improving the quality of electronic fetal monitoring.

JIRI KOZIOREK was born in Czech Republic, in 1973. He received the master's degree in measurement and control systems from the Faculty of Electrical Engineering and Computer Science, VSB—Technical University of Ostrava, in 1996. Since 1998, he has been an Assistant Professor with VSB—TU Ostrava. During his Ph.D. study, he is working in the area of distributed control system design. He defended his Ph.D. thesis in technical cybernetics, in 2005. In 2008, he became an Associate Professor in the field of technical cybernetics. Since 2009, he has been the Head of the Department of Cybernetics and Biomedical Engineering, VSB—TU Ostrava. He is a Coordinator of several national and international research projects typically in cooperation with industrial partners. His research interests include control system design, industrial communication, digitalization of industry, sensors, and non-electrical measurement.